The Thesis Committee for Xiwei Yan Certifies that this is the approved version of the following thesis:

Investigation of the Proteomic Interaction Profile of Uncoupling Protein 3 and its Effect on Epigenetics

APPROVED BY
SUPERVISING COMMITTEE:

Supervisor : _____
Edward M. Mills

_____
Casey Wright

Investigation of the Proteomic Interaction Profile of Uncoupling Protein 3 and its Effect on Epigenetics

By

Xiwei Yan, B.S.; B.S.

Thesis

Presented to the Faculty of the Graduate School of
The University of Texas at Austin
in Partial Fufillment
of the Requirements
for the Degree of

Master of Arts

The University of Texas at Austin
August 2014

Acknowledgements

I would like to thank my mentor Dr. Edward Mills for his guidance and support through this project and during my two years in his laboratory. Dr. Mills has given me lots of help and encouragement on both the research and my career planning. I have learned from him not only knowledge, but also the positive attitude for life from. I sincerely hope that my work can contribute to the success of his laboratory.

I would also like to thank the current and past laboratory members of the Mills lab for their help and support. When I joined the lab with little research experiences, they patiently taught me a lot about the lab techniques, and generously tolerated all the mistakes I have made. I would especially like to thank Christine Dao and Gloria Fang. Christine has helped me a lot with the proteomics experiment. Without her, the experiment may not be as successful as it turned out to be. Gloria always gave me the most detailed instructions on the lab techniques used in my project. And all the other lab members have given precious suggestions whenever I had questions. I feel very lucky to meet them and have them as my colleagues.

Finally, I would like to thank my parents and friends for their understanding and support through my graduate school.

Investigation of the Proteomic Interaction Profile of Uncoupling Protein 3 and its Effect on Epigenetics

Xiwei Yan, M.A.
The University of Texas at Austin, 2014

Supervisor: Edward M. Mills

Uncoupling proteins (UCPs) are a family of highly conserved proteins that is located on the inner mitochondrial membrane (IMM) and "uncouple" the electrochemical proton gradient formed by the electron transport chain (ETC) from ATP production. The first discovered uncoupling protein 1 (UCP1) is generally believed to mediate the proton leak-dependent thermogenesis in rodents and human neonates, but the physiological and biochemical functions of the homologs UCP2-5 are still under debate.

Our research focuses on UCP3, the homolog prevalently expressed in skeletal muscle (SKM), and also detected in heart, BAT and other smooth-muscle containing organs at lower levels. Since skeletal muscle and heart are important metabolic organs, UCP3 has long been speculated to have a pivotal role in maintaining the mitochondrial metabolism. Several biochemical roles have been attributed to UCP3, including the regulation of fatty-acid transport and oxidation, reactive oxygen species (ROS) scavenging and calcium uptake. And several proteins have been identified to directly bind with UCP3 and facilitate its function. But to further understand how UCP3 relates to different aspects of mitochondrial functions, a more comprehensive profile of the UCP3 interaction partners is needed. The data I obtained from the mass spectrometry-based experiment successfully gave a list of over 170 potential proteins that may directly or indirectly interact with UCP3, and several novel functions of UCP3 are implied by these protein-protein interactions.

Additionally, researches have shown that the metabolic defects (including the accumulation of ROS and certain metabolites) are important contributing factors to the epigenetic changes. Considering the biochemical roles of UCP3 in sustaining the normal mitochondrial metabolism, we hypothesize that UCP3 has a novel function in regulating the genomic DNA methylation processes, and the loss of UCP3 will lead to aberrant DNA methylation changes. The data I obtained from the pilot study confirms this hypothesis and indicates the potential role of UCP3 in maintaining normal epigenetic marks. But further experiment is still needed to investigate the regulatory pathway between UCP3 and DNA methylation.

The physiological role of UCP3 in defending against cancer, diabetes and obesity has been discussed, but the mechanisms how UCP3 protect the organism from these diseases have not been elucidated. Since the occurrences of these diseases are always characterized by aberrant epigenetic marks and altered metabolism, and understanding of UCP3 functions may be of significant therapeutic benefit in the prevention and treatment of these diseases.

Table of Contents

List of Figures

List of Tables

Chapter 1 Introduction

1.1 Mitochondrial Metabolism

The mitochondrial respiration pathways are conserved in almost all living organisms. Compared to glycolysis, it is much more efficient in generating adenosine triphosphate (ATP), the high-energy intermediates used in the majority of biological processes. In this sense, the mitochondria are responsible for fueling the cellular energy demands for most of the time.

The biochemical reactions happened in the mitochondria are very complicated. The most well-known pathways are the tricarboxylic acid (TCA) cycle and the electron transport chain (ETC), but other reactions (including the fatty-acid oxidation, the folate cycle pathway, and apoptosis) are also crucial in the normal function and even survival of cells. This thesis will focus primarily on the TCA cycle and ETC, but will also involve some of the other reactions in later sections.

1.1.1 The Mitochondrion

Mitochondria are membranous organelles existing in almost all eukaryotic cells. According to the “Endosymbiotic Theory”, mitochondria originated from symbiosis between different prokaryotic cells. After millions of years of evolution, mitochondria have become highly-specialized and indispensible organelles that primarily focus on energy production.

The mitochondrial space is separated by two phospholipid membranes, resulting in four distinct compartments: the outer mitochondrial membrane (OMM), intermembrane space, the inner mitochondrial membrane (IMM), and the matrix. The outer mitochondrial membrane encloses the entire organelle and is fully permeable to small molecules due to a large number of porin channels. The intermembrane space is the compartment between the outer and inner

membranes. Due to the permeability of the OMM, the intermembrane space has similar small molecule concentrations as the cytoplasm. The inner mitochondrial membrane contains a high density of proteins, including various transporters and the complexes in the electron transport chain (ETC), which is responsible for the majority of ATP production in the cell. Meanwhile, the IMM is highly impermeable due to the absence of porin channels, and this property maintains the proton gradient that is necessary for mitochondrial functions. The matrix is the compartment where TCA cycle and many other mitochondrial enzymatic reactions take place. It is able to provide the electron donors (NADH and $FADH_2$) that are necessary for the electron transport chain to operate. Because of the importance of ATP production in cell metabolism, the number of mitochondria is always correlated with the cellular metabolic level. For example, the highly metabolic organs such as muscle and liver can contain hundreds of mitochondria. And research has shown that exercises can further induce the biogenesis of mitochondria in skeletal muscle to meet the increased energy demand (Hood, 2009).

1.1.2 The Citric Acid Cycle

Carbohydrate is the most common food substrate in human diet. After its consumption, the digestive system breaks it down to glucose before entering the cell. Then the glucose is transported into the cell by the GLUT transporters, and finally be used to produce large amount of ATP through the citric acid cycle (also known as TCA cycle) and oxidative phosphorylation (Moreno-Sánchez et al., 2007).

The first few steps of glucose catabolism are called glycolysis, which occur in the cytoplasm. Glucose is modified and decomposed by a series of steps, and eventually produces two pyruvate and two ATP molecules per glucose used. There are usually two outcomes for the resulting pyruvate: (1) in the absence of oxygen (as muscle cells under condition of anaerobic exercise) or absence of

mitochondrion (as in the red blood cells), the pyruvates are converted to two molecules of lactate by the lactate fermentation in the cytoplasm; (2) in the presence of both oxygen and mitochondrion, the pyruvates are shuttled to the mitochondrial matrix where they are cleaved to form acetyl-CoA.

Then Acetyl-CoA enters the TCA cycle by reacting with oxaloacetate to produce citrate. Citrate is then in turn converted to isocitrate, α-ketoglutarate, succinate, fumarate, malate and back to oxaloacetate by a series of reactions, and this oxaloacetate is able to combine with another molecule of acetyl-CoA and initiating another cycle of reactions (Figure 1.1). Through each cycle, two molecules of nicotinamide adenine dinucleotide (NADH) and 1 molecule of flavin adenine dinucleotide ($FADH_2$) are generated and fed into the electron transport chain as the electron donors (Wolfe and Jahoor, 1990).

1.1.3 The Electron Transport Chain and Oxidative Phosphorylation

The electron transport chain (ETC) passes electrons to the final electron acceptor oxygen, and simultaneously pump proton out of matrix to form membrane potential. ETC includes four major complexes that are embedded in the inner mitochondrial membrane. The cofactors NADH and $FADH_2$ produced from the TCA cycle deliver their electrons to complex I and II, respectively, then the electrons are shuttled to mobile lipophillic carrier ubiquinone to complex III to cytochrome C to complex IV. The electrons reduce molecular oxygen at complex IV and produce water in the matrix. Meanwhile, the passing of electrons leads complexes I, III and IV to actively pump 4, 2, and 4 protons respectively into the intermembrane space, contributing to the formation and maintenance of the proton gradient across the inner membrane (Rottenberg, 1975). This membrane potential provides the proton motive force that powers the ATP production. By passing protons back into the matrix along the concentration gradient, the F_1/F_0 ATP synthase, also known as complex V, utilizes this proton motive force to produce 34 molecules of ATP molecules for each glucose molecule metabolized.

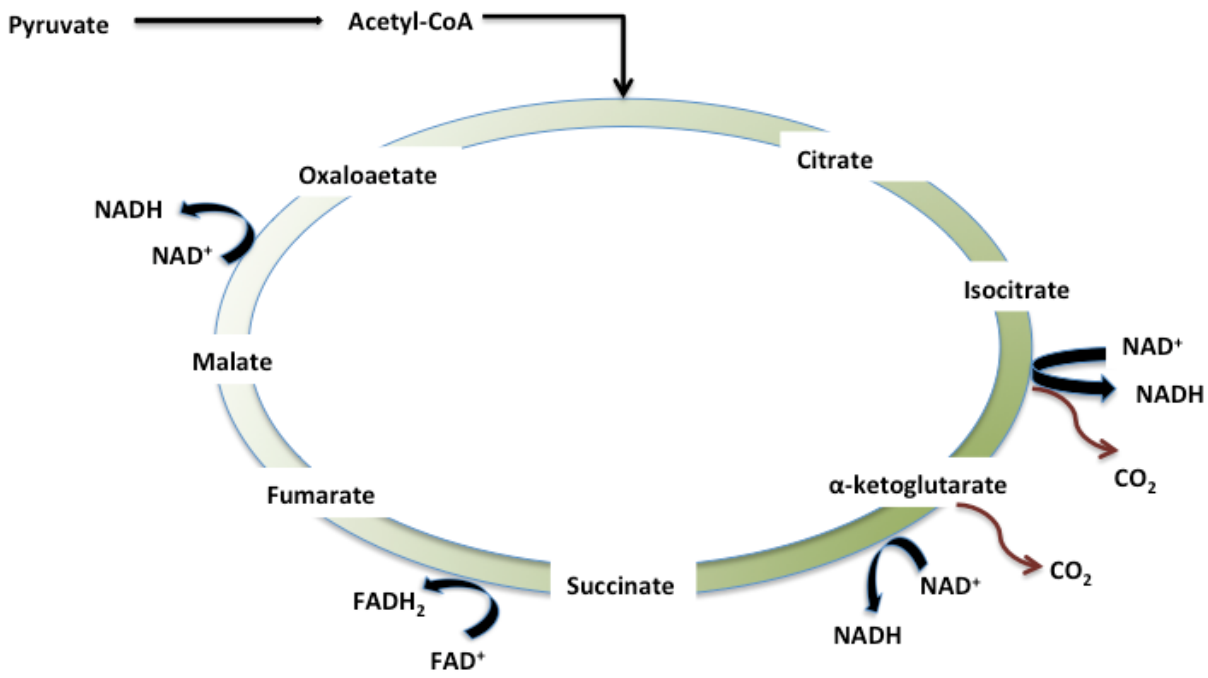

Figure 1.1 The Citric Acid Cycle. The Citric acid cycle Includes complicated enzymatic reactions during which 1 molecule of acetyl-CoA is consumed, while 2 molecules of NADH and 1 molecule of FADH2 are produced.

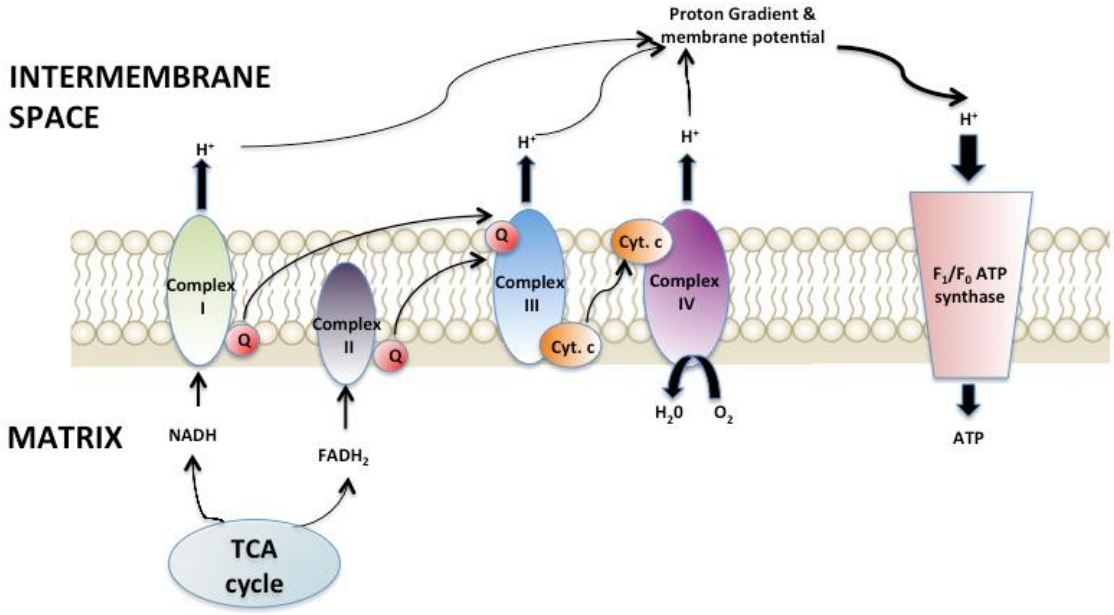

Figure 1.2 The Electron Transport Chain and Oxidative Phosphorylation. Cofactors NADH and $FADH_2$ deliver electrons to complex I and complex II, which transfer the electrons to complex III through ubiquinone. From complex III the electrons are transferred to cytochrome c (Cyt. C) and finally to complex IV. At complex IV the electrons are oxidized by molecular oxygen and produce water. Meanwhile, the protons pumped out by complex I, II and IV are used to form the membrane potential and drive the F_1/F_0 ATP synthase to produce ATP.

This is the process called oxidative phosphorylation (OXPHOS) (Figure 1.2) (Boyer, 1997; Schultz and Chan, 2001).

1.2 Mitochondrial Respiratory Efficiency

As previously mentioned, the oxidative phosphorylation is very efficient in generating ATP, producing 34 ATPs in the ideal situation. However, the proton leaking though the inner mitochondrial membrane uncouples the proton gradient from ATP synthesis. Namely, not every proton pumped into the intermembrane space is used for ATP production, which makes the ATP synthesis via OXPHOS less efficient,

In the situation when the cell has abundant ATP, the ATP synthase will be inhibited by the high ATP/ADP ratio and slow down the ATP production. In turn, electron transport rate and therefore respiration slows, membrane potential is elevated, and the tendency of electrons to slip from complexes I,II and III is increased. Therefore, the reactive oxygen species (ROS) form when the escaped electrons attack O2 molecules and partially reduce them.

To prevent the damages caused by ROS, mitochondrial membranes developed several mechanisms to leak protons, thereby decreasing the proton gradient and making oxygen consumption operate normally even in the absence of ATP production (Brand and Esteves, 2005). This process is termed respiratory uncoupling because it dissipates the proton gradient formed by the electron transport chain. As the result, the electron transport chain drives wasted cycles of proton pumping and proton leaking, and release the energy in the form of heat (Figure 1.3) (Cannon and Nedergaard, 2004).

This basal proton leak is shown to be responsible for about 20-50% of the total cellular respiration rate in rat skeletal muscle and liver (Rolfe et al., 1999). This unexpectedly high uncoupling rate implies the importance of maintaining a consistent membrane potential and normal operation of the electron transport

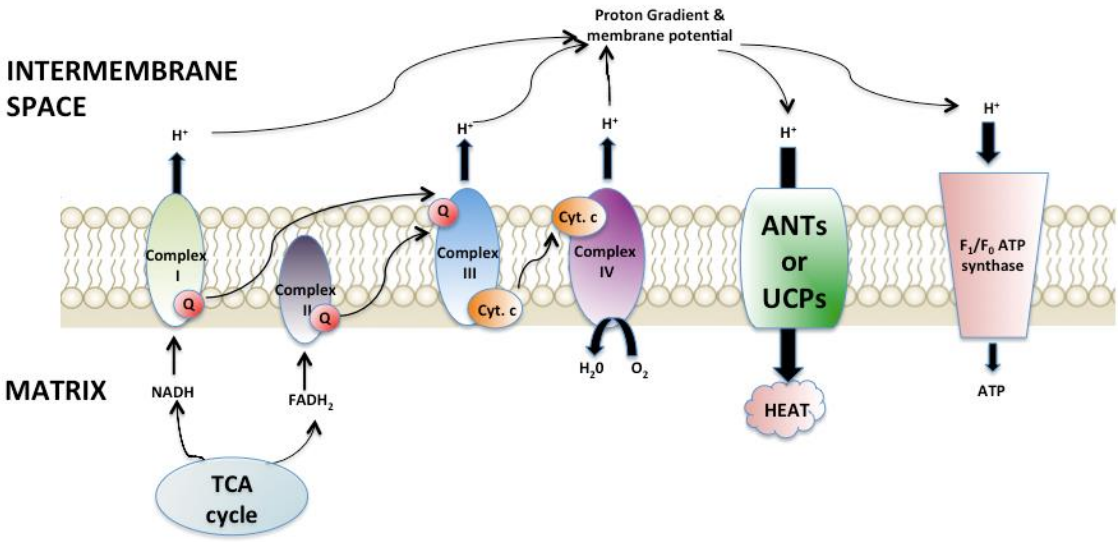

Figure 1.3 The Mechanism of Respiratory Uncoupling. ANTs and UCPs mediate basal and induced respiratory uncoupling respectively. The mechanism of uncoupling is to dissipate the proton gradient formed by the electron transport chain and decrease membrane potential. Through this process, the proton gradient is uncoupled from ATP production, while the energy is released as heat.

chain, even without the energy demand to produce ATP.

There are several mechanisms responsible for the respiratory uncoupling processes under different conditions. For the basal proton leak mentioned above, a small proportion is due to the diffusion across the mitochondrial membranes, and the majority of basal proton conductance (~64%) is conducted by the adenine nucleotide translocase (ANT) (Brand and Esteves, 2005; Parker et al., 2008). ANTs are a group of Mitochondrial Carrier proteins localized in the inner mitochondrial membrane. Their main function is to use the proton motive force export ATP from the matrix in trade for cytoplasmic. In addition to the basal proton conductance, mitochondria also have an inducible proton leak route mediated through the uncoupling proteins (UCPs), which promote around 11% of the uncoupling in mammalian tissues (Parker et al., 2008). Studies using UCP-knockout mice have shown that UCPs are not responsible for the basal proton leak across the inner mitochondrial membranes (Brand and Esteves, 2005). On the contrary, their activity can be activated or inhibited by some common metabolites in the mitochondrial environment, enabling UCPs to respond quickly to the changes in the metabolic level in mitochondria.

1.3 Mitochondrial Uncoupling Proteins

Uncoupling proteins are evolutionarily conserved carrier proteins that belong to the mitochondrial solute carrier superfamily (SLC25) of transporters. All SLC25 transporters are nuclear-encoded and localized to the inner mitochondrial membrane, responsible for transporting various solutes between the mitochondrial matrix and cytoplasm. The members of the SLC25 family are very similar in structure. They all contain six trans-membrane domains, with the N- and C-termini in the intermembrane space (Figure 1.4) (Maloney, 1990). They are also predicted to have FA binding domains, nucleotide binding domains, and pH sensing domains (Robinson et al., 2008). There are 27 SLC25 family

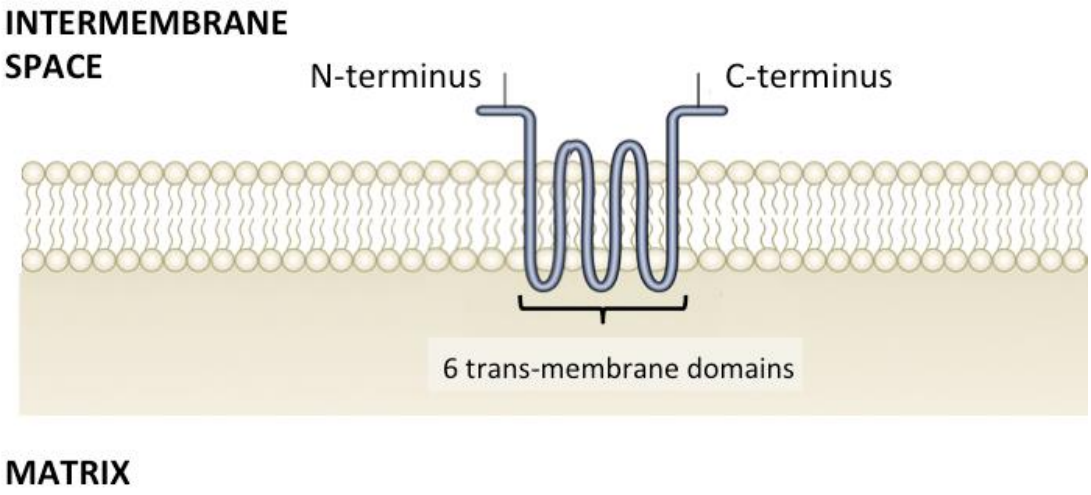

Figure 1.4 Domain Structures of UCPs and other SLC25 Family Proteins.
The SLC25 family proteins are localized in the inner mitochondrial membrane. All of them contain seven hydrophilic domains connected by 6 trans-membrane domains.

members identified to date, including the ANTs, another group of proteins mediating proton leak mentioned in the previous section.

The UCPs comprise the largest subfamily of SLC25. This subfamily includes five identified trans-membrane anion-carrier proteins (UCP1-5), each having distinct physiological implications and expression patterns (Krauss et al., 2005). Their roles are generally associated with regulation of proton conductance across the inner mitochondrial membrane and maintaining the normal level of mitochondrial respiration. As opposed to the basal proton leak, the uncoupling mediated by UCPs is inducible but strongly inhibited. UCPs are strongly inhibited by purine nucleotides (including ADP and GDP), which bind at the intermembrane side of UCPs (Echtay et al., 2003; Jabůrek and Garlid, 2003). Meanwhile, several activators of UCPs have been identified, although the mechanism how these molecules regulate UCPs is still unclear. The most common type is medium to short-chain fatty acids, including lauric, palmitic, capric, oleic, and linoleic acids (Jabůrek and Garlid, 2003; Ježek et al., 1997). The binding of fatty acid with UCP induces conformational changes that can mask the nucleotide-binding domains, and therefore overcome the inhibition by the nucleotides (Huang, 2003). In addition to fatty acids, superoxide (O_2^-) and lipid peroxides that produced from oxidation of FFAs are also able to activate UCPs through covalent modification (Echtay et al., 2002, 2003; Esteves and Brand, 2005; Talbot et al., 2003, 2004).

The biochemical mechanism by which UCPs mediate uncoupling is still under debate. A few mechanisms have been hypothesized, but by far no conclusion is reached (Figure 1.5). One model is that UCPs directly transport protons from the inner membrane space to the matrix and use fatty acids as cofactors to facilitate the proton leak (Garlid et al., 1998; Klingenberg and Huang, 1999). The second model is that UCPs act as OH^- uniporter, which is allosterically activated by fatty-acid (Nicholls, 2006). The third model is referred as “fatty-acid cycling” model, in which UCPs act as antiporters for protonated/unprotonated fatty acids and transport protons indirectly. In this process, fatty acids are protonated in the more acidic intermembrane space, imported by UCP into matrix, deprotonated, then

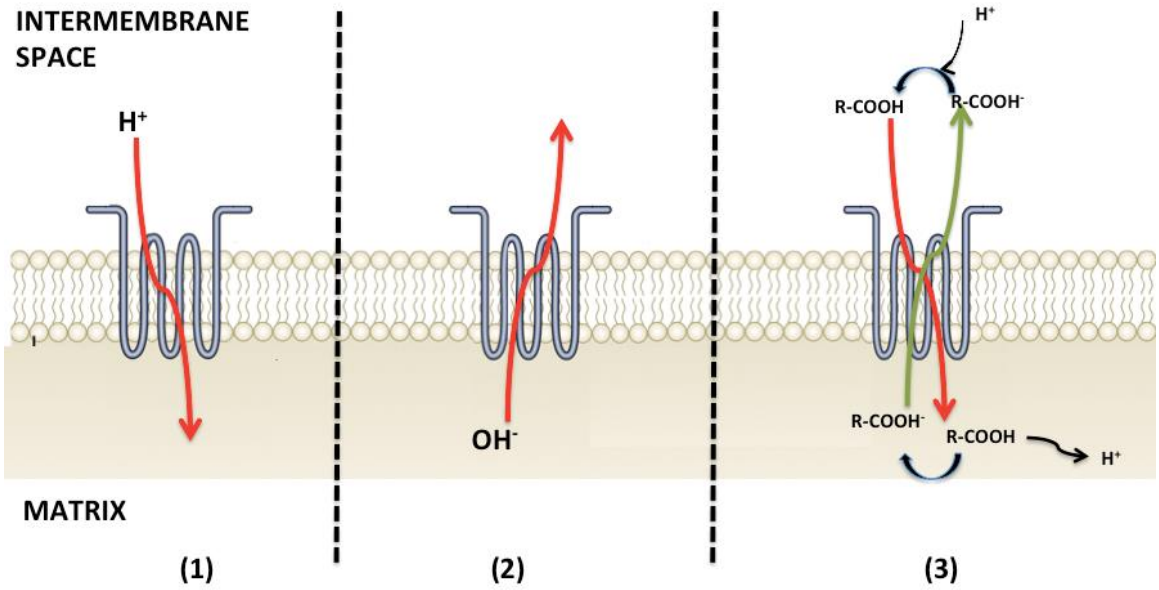

Figure 1.5 The Proposed Models of UCP-mediated Proton Leak. There are three theories about this process: (1) suggests UCP directly translocate proton into the matrix as an uniporter; (2) suggests UCP transport hydroxyl group out of the matrix, which is electrochemically equivalent to importing a proton; (3) suggests UCP transport fatty acid anion out of the matrix, where the anion gets protonated and then transported back into the matrix, then the proton dissociates from the fatty acid. Through this "fatty acid cycling" model, the proton is transported into the matrix.

translocated into intermembrane space again. In this model, the uncoupling protein facilitates the exchange of one protonated fatty acid for one unprotonated fatty acid, resulting in leaking of proton into matrix without changing fatty acid level on either side (Ježek et al., 1998; Porter, 2008).

In summary, all UCPs facilitate proton leak back into the matrix, thereby lowering the mitochondrial membrane potential generated by ETC. This process uncouples the electron transport from ATP production, which means it drives electron transport and oxygen consumption without ATP synthesis, and releases the energy as heat.

1.3.1 Uncoupling Protein 1

UCP1 is the first member discovered in the UCP family, and is well-known for its role in brown adipose tissue (BAT) thermogenesis. BAT is a distinct type of adipose tissue from the more commonly found white adipose tissue (WAT). Compared with the simple fatty-acid-storage function of WAT, BAT has a more energy-demanding role – maintaining the body temperature, especially in neonates and hibernating animal (Smith and Horwitz, 1969). The structural and functional analysis of BAT demonstrated that BAT contains a much higher amount of mitochondria, and the mitochondria isolated from BAT exhibited an unexpectedly high level of respiration (Hittelman et al., 1969; Smith and Horwitz, 1969).

UCP1 was first identified in isolated mitochondria from BAT in 1970's, and the excessively high respiratory capacity of BAT is attributed to UCP1 (Bouillaud et al., 1985; Cannon et al., 1982; Nicholls, 1976). Numerous investigations have been performed since its discovery, and have gained remarkable insight in respect of its expression pattern, function and regulation.

UCP1 is traditionally believed to express exclusively in BAT of rodents, infant humans and hibernating mammals. However, BAT depots are recently identified

in adult humans, and UCP1, as the identifying marker of BAT, is also present (Nedergaard et al., 2007). UCP1 is much more abundantly expressed in BAT than any other UCPs, accounting for up to 10% of the mitochondrial protein expression (Nicholls, 1976). Consequently, it is considered the primary uncoupling protein in BAT, where its effect cannot be masked by other homologs (Cannon and Nedergaard, 2004; Parker et al., 2009).

UCP1 has been shown to dissipate the proton gradient across the mitochondrial inner membrane and increased heat production in mitochondrial matrix. Because of its uncoupling properties, UCP1 is implicated in the regulation of respiration and diet-induced thermogenesis. Genetic inactivation of UCP1 in mice results in the defective cold-induced thermogenesis, confirming the physiological role of UCP1 in BAT thermogenesis (Enerbäck et al., 1997; Feldmann et al., 2009). But whether UCP1 is associated with body weight regulation is still unclear, due to conflicting experimental results (Nedergaard et al., 2007).

As a prototypical UCP, the activity of UCP1 is strongly inhibited by purine nucleotides at physiological level and activated by free fatty acid (Huang, 2003; Nicholls, 1976). At the histological level, UCP1 is tightly regulated by stimuli such as diet and cold stress. Under these conditions, the adrenergic receptors on the cell surface are activated and result in increased cellular free fatty-acid level, which will activate UCP1 mediated proton conductance within minutes (Klaus et al., 2001; Rodriguez-Cuenca et al., 2002).

1.3.2 Uncoupling Protein Homologs

The uncoupling proteins are a subfamily of the mitochondrial solute carrier proteins that have been found in fungi, plants, protists, insects, nematodes, flies, and vertebrates (Iser et al., 2005; Ježek et al., 1996; Sanchez-Blanco et al., 2006). Since the discovery of UCP1 in 1976, other homologs have been identified based upon their protein sequences (UCP1-5). Though extensive

researches have been performed on these homologs, UCP1 is by far the only UCP that has a well-established physiological function. All these homologs have distinct expression patterns, and have been involved with various tissue-specific physiological roles.

UCP2 was first identified in 1997 and is ubiquitously expressed in mammalian tissues at varing levels (Fleury et al., 1997; Mattiasson and Sullivan, 2006). Although it has the highest sequence homology (59%) to UCP1, it is functionally distinguishable from UCP1 (Fleury et al., 1997). Unlike UCP1, genetic ablation of UCP2 in mice has not affected the cold-induced thermoregulatory capacity (Matthias et al., 2000). However, UCP2 has shown a more indirect function in thermoregulation by increasing the sensitivity of the nervous system to the thermoregulatory hormone triiodothyronine (Coppola et al., 2007; Zaretskaia et al., 2002). UCP2 also plays a physiologically important role in regulating the glucose-stimulated insulin secretion and defending against type-2 diabetes. The pancreatic β-cells can detect the blood glucose level and secret insulin when its concentration is high. In this process, the cellular ATP/ADP ratio acts as the indicator of the blood glucose level (Rutter, 2001). Through its uncoupling function, UCP2 dissipate the proton gradient formed by ETC and decreases ATP production derived from glucose metabolism. Thus, UCP2 maintains a relatively low ATP/ADP ratio in β-cells and negatively regulates insulin secretion (Chan et al., 1999, 2001; Zhang et al., 2001). This model is supported by genetic engineering of UCP2 in animal and cell line. When overexpressed, UCP2 further attenuates glucose-stimulated insulin secretion in pancreatic β-cells (Li et al., 2001). But the UCP2 knockout mice showed significantly increased insulin secretion from pancreatic islets (Zhang et al., 2001).

UCP3, the focus of this thesis, is also identified in 1997. UCP3 also shows high sequence homology (57%) to UCP1, but their expression patterns are vastly different (Boss et al., 1997). UCP3 is primarily expressed in skeletal muscle and to a lesser degree in heart and BAT (Boss et al., 1998; 2000; Vidal-Puig et al.,

1997; Clapham et al., 2000). Most recently, UCP3 has been found in human pancreatic islets (Li et al., 2008) and human skin (Mori et al., 2008). UCP3 shares conserved structure with UCP1, including the domains responsible for proton leak and nucleotide binding. Thus, UCP3 is speculated to have similar roles as UCP1. However, in addition to thermogenesis, different biological processes have been associated with UCP3, including insulin secretion, redox regulation, fatty-acid transport and metabolism, but no consensus has been reached to date. These will be discussed in later sections.

Compared to UCP1-3, relatively little is known about the neuronal UCPs, UCP4 and UCP5. Comparative analysis of amino acid sequences shows that UCP4 and UCP5 share the least sequence homology (~31%) with UCP1, and has been postulated to act through different biochemical mechanisms, rather than the classical uncoupling function (Mattson and Liu, 2003; Palmieri, 2004).

UCP4 is expressed in nearly all areas of the brain, and at low levels in the spinal cord (Mao et al., 1999). The expression of UCP4 in brain is developmentally regulated, as the level of UCP4 is elevated along with neuronal differentiation (Smorodchenko et al., 2009). Statistical study has also implied an involvement of UCP4 with the etiology of schizophrenia (Yasuno et al., 2007). These results indicate that UCP4 has a specific function in neuronal development. Besides, ceUCP4, which is highly similar with hUCP4, has shown a novel biochemical function in regulating mitochondrial succinate import (Pfeiffer et al., 2011). In this way, it is able to regulate the mitochondrial respiration and glucose metabolism without changes in the uncoupling level. UCP4-5 share the same inhibitors (purine nucleotides) as mammalian UCP1-3, but are not responsive to the common activating agent of UCPs, the free fatty acid (Ivanova et al., 2010; Jabůrek and Garlid, 2003). Comparative sequence analysis revealed that UCP4 lacks several key residues responsible for FA binding and proton transport (Robinson et al., 2008). This again implies that UCP4 may not function as a classical uncoupler. However, UCP4 still retains at least part of the classical uncoupling functions, as the overexpression of UCP4 in neural cells has been

demonstrated to decrease the membrane potential, reduce reactive oxygen species level and decrease mitochondrial calcium accumulation (Liu et al., 2006). Since the brain has a high-metabolic demand and highly relies on glucose as the energy source, it is likely that UCP4 serves as an important regulatory protein under conditions of metabolic and oxidative stress. Moreover, Mutations in UCP4 have been related to the aging-associated diseases, such as Alzheimer's disease and Parkinson's disease, confirming the importance of UCP4 in protecting the brain against the oxidative stress (Wu et al., 2009). Since Ca^{2+} acts as an key secondary messenger in controlling oxidative phosphorylation and apoptosis, the ability of UCP4 to regulate Ca^{2+} accumulation in mitochondria via reducing membrane potential is also physiologically crucial.

UCP5, also known as brain mitochondrial carrier protein-1 (BMCP1), is expressed in specific brain regions such as the cortex, hippocampus, and thalamus (Kim-Han et al., 2001; Sanchis et al., 1998). Very little is known concerning UCP5 function, but it has been observed to function as a prototypical uncoupling protein and decrease membrane potential (Yu et al., 2000). This mechanism implicates its ability to decrease ROS production in the brain. Recently, a UCP5 homolog in Drosophila was identified to be related to energy homeostasis and aging (Sanchez-Blanco et al., 2006).

1.3.3 Uncoupling Protein 3

When UCP3 was first identified in 1997, it was found to have has high sequence homology and structural resemblance to UCP1. Considering it is expressed mainly in the highly thermogenic and metabolic tissues (skeletal muscle, brown adipose tissue, and heart), UCP3 is speculated to have the same thermogenic function as UCP1 (Boss et al., 1997). Several studies support this model, as increased UCP3 expression has been observed in response to cold exposure, and absence of UCP3 leads to abolished drug-induced hyperthermia (Larkin et al., 1997; Mills et al., 2003). However, there is also evidence against this model.

The identification of UCP homologs in ectotherms such as fish and plant seems to imply UCPs have some different and more general function (Laloi et al., 1997; Stuart et al., 1999). Moreover, UCP3-deficient mice showed normal cold-induced thermogenesis, although decreased muscle proton leak was observed (Golozoubova et al., 2001; Gong et al., 1997). Thus, although the exact functions of UCP3 mediated are still unclear, it is a consensus that the thermogenesis is not the primary role of UCP3.

The biochemical functions of UCP3 have been investigated in numerous studies. One of the most well-known models proposed is the mitigation of oxidative stress. This function has been confirmed by the In vivo study that showed decreased ROS-induced protein damage in skeletal muscle when UCP3 was overexpressed (Barreiro et al., 2009). As previously mentioned, ROS forms when the electron transport chain slows down and electrons slip away from ETC. ROS are generally believed to be toxic as they can damage proteins, DNA, and lipids, and have been connected to many diseases. The model hypothesizes that: Since UCP1-3 can be activated by superoxide as previously mentioned, the accumulation of ROS can promote UCP3 to drive the electron transport and oxygen consumption, and in turn reduce ROS production (Figure 1.6). As the uncoupling function is common for the whole UCP family, this role in redox regulation has also been observed from all other UCPs (Korshunov et al., 1997). Another ROS scavenging protein, thioredoxin 2 (Trx2) has been identified as a direct interaction partner of UCP3, and facilitates the UCP3-dependent suppression of ROS production (Hirasaka et al., 2011).

The second proposed function of UCP3 is the regulation of insulin secretion in pancreatic islet cells. Insulin resistance in skeletal muscle is the major cause of Type 2 diabetes mellitus (T2DM), the most common form of diabetes (Chan and Harper, 2006). Evidence supporting the function of UCP3 in ameliorating insulin resistance comes from studies showing that mice overexpressing UCP3 in skeletal muscle are protected from obesity and insulin resistance (Choi et al., 2007; Son et al., 2004). A mechanism trying to explain this protective role of

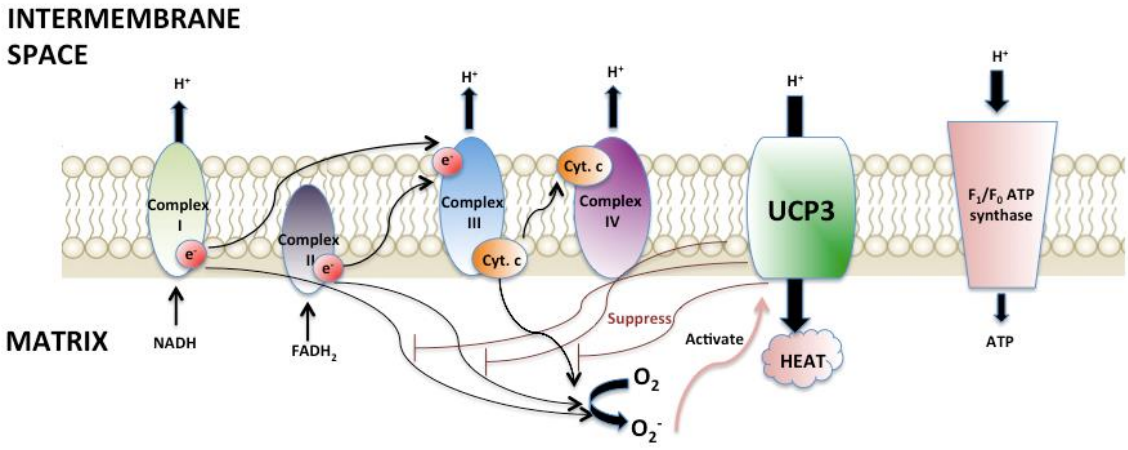

Figure 1.6 The Mechanism of UCP3-mediated ROS Suppression. When protons accumulate in the intermembrane space, ETC slows down and electrons slip away from complex I, II and III to attack molecule oxygen. The molecule oxygen gets partially reduced and form superoxide, which can activate UCP3. Once activated, UCP3 dissipates the proton gradients and reduces membrane potential. This drives the electron transport and prevents electrons from slipping away from ETC.

UCP3 is proposed by Li et al, who identified UCP3 in pancreatic islet cells and found it to participate in insulin secretion regulation (Li et al., 2008).

Besides, the role of UCP3 in the regulation of fatty acid metabolism and transport also seems important to the prevention of obesity and diabetes. Studies have demonstrated involvement of UCP3 in nonesterified fatty acids transport from the mitochondrial matrix into the intermembrane space (Schrauwen et al., 2001, 2006). As the accumulation of fatty acid can activate UCP3, this function is believed to prevent lipotoxicity by exporting the excess fatty acids and facilitate β-oxidation and the TCA cycle by liberating coenzyme A (Himms-Hagen and Harper, 2001). The animal model supports this mechanism as overexpression of UCP3 in mice has shown increased level of fatty acid transport and oxidation(Bézaire et al., 2007; Bezaire et al., 2005). Our lab has proposed another mechanism by which UCP3 regulate fatty acid metabolism. UCP3 is shown to directly bind $\Delta^{3,5}\Delta^{2,4}$dienoyl-CoA isomerase (DCI), an auxiliary fatty acid oxidation enzyme specifically for unsaturated fatty acid with odd-numbered double bond, such as linoleic, linolenic and oleic acid. Without DCI, these unsaturated fatty acids cannot be oxidized and will accumulate in mitochondrial as toxic lipid metabolites. The interaction between UCP3 and DCI has been proven to promote the oxidation of these acids (unpublished).

Other functions are less discussed but have also been proposed. One of the models is the function of UCP3 in regulating mitochondrial Ca^{2+} uniport, the key regulator of apoptosis (Graier et al., 2008). In this model, UCP3 is believed to mediate Ca^{2+} import independent of Ψ, which indicates UCP3 may catalyze additional biochemical reaction other than proton leak (Trenker et al., 2007).

More recently, another study has shown that UCP3 can drive cell differentiation and oppose cancer development in mouse keratinocytes through unclear mechanisms (Lago et al., 2012).

In summary, although all these different functions of UCP3 have been proposed and debated, no conclusion is reached to date.

1.4 UCP3 and DNA methylation

Epigenetics defined as heritable changes in gene expression that occur without changes in DNA sequence (Li et al., 2005). It generally refers to DNA methylation and histone modifications (including phosphorylation, acetylation, methylation, ubiquitylation etc.), which are recently revealed to be interdependent and bidirectionally crosstalking (Cedar and Bergman, 2009). DNA methylation is traditionally believed to be stable against environmental factors. However, dynamic methylation changes are later found to be associated with various diseases, environmental stresses, and even exercise (Barrès et al., 2012; Weber et al., 2005). The most typical aberrations of DNA methylation occur at 5-carbon of cytosine in CpG islands, which is catalyzed by DNA methyltransferases (DNMT). In mammalian cells, three DNMTs exist to mediate CpG hypermethylation: DNMT1 maintains the large degree of global DNA methylation, whereas DNMT3A and DNMT3B are *de novo* methylases that are responsible for the dynamic methylation (Li, 2002).

Previous researches have shown quite some examples that dysfunctional mitochondrial respiration abolishes the balance of epigenetic control. Some metabolites accumulated during defective TCA cycle, including the 2-hydroxyglutarate, succinate and fumarate, have shown specific inhibitory effects on enzymes mediating DNA demethylation and histone demethylation (Cervera et al., 2009; Chowdhury et al., 2011; Figueroa et al., 2010; Turcan et al., 2012; Xiao et al., 2012; Xu et al., 2011). Moreover, the absence of mitochondrial DNA has been shown to significantly induce DNA methyltransferase 1 and result in global hypermethylation of the genomic DNA (Xie et al., 2007).

By far, there are very few researches investigating the relationship between UCPs and Epigenetics, except one study showing that UCP1 is regulated by histone demethylase Jhdm2a (Tateishi et al., 2009). However, many diseases that UCP3 defend against, including cancer, obesity and type II diabetes, are tightly coupled with altered metabolism and methylation-dependent silencing

of specific genes. In addition, normal mitochondrial metabolism is required for the maintenance of normal epigenetic processes. Considering the crucial function of UCP3 in driving the electron transport and mitochondrial respiration, as well as in suppressing ROS generation and facilitating fatty acid oxidation, the absence of UCP3 may lead to dysregulated epigenetics, and consequently various diseases.

Given the role of UCP3 in relieving oxidative stress, reactive oxygen species provide a potential link between UCP3 and epigenetics. ROS have been shown to play opposite roles in inducing both DNA hypermethylation and hypomethylation (Donkena et al., 2010). On one side, ROS has been found to alter DNA methylation by oxidizing DNMTs or through direct oxidation of nucleotide. Additionally, the cofactor S-adenosyl methionine (SAM), which is the methyl donor for DNA methylation and histone methylation, is also dependent on the glutathione metabolism. When glutathione is depleted by ROS, methyl donors become deficient, resulting in genome-wide DNA hypomethylation (Hitchler and Domann, 2009; Naviaux, 2008). On the other side, ROS-induced DNA hypermethylation of promoter CpG islands is a very frequent mechanism for gene expression inhibition, and is frequently seen in tumors (Quan et al., 2011). Previous studies have shown the ability of ROS to induce gene promoter hypermethylation by enhancing DNMT expression, activity and recruitment to the promoter regions (He et al., 2012; Kang et al., 2012; Lim et al., 2008).

The only experiment trying to investigate the connection between proton leak and DNA methylation is performed using FCCP, a chemical uncoupler. Unfortunately, the cell cannot survive long enough with FCCP treatment, and they failed to observe a change in methylation level (Xie et al., 2007). However, the model that DNA methylation is affected by mitochondrial respiratory uncoupling is still plausible and requires further investigation.

1.5 Concluding Remark

Mitochondrial uncoupling proteins are the principle mediator of inducible proton leak in various tissues. The prototypical UCPs can increase mitochondrial respiration by driving the flux of electron transport and promoting the reduction of oxygen. Due to the importance of respiration and glucose metabolism in all organisms, UCPs are speculated to have crucial roles in keeping the energy balance and mitochondrial metabolism. Among the members in the UCP family, only UCP1 has a well-established function in maintaining body temperature. All the other UCPs (UCP2-5) are still in mystery. UCP3 has been implicated in ROS mitigation, fatty acid export, and calcium uptake, but no conclusive answer has been widely accepted.

Several proteins have been found to interact with UCP3 and facilitate different UCP3 functions, while more protein-protein interactions involving UCP3 have been observed but need to be confirmed by biochemical approaches. Based on these results, our hypothesis is that UCP3 form a well-organized multi-protein complex with different proteins, and carry out more roles than simply mediate respiratory uncoupling. To prove this hypothesis, we need a more comprehensive profile of proteins interacting with UCP3, the interaction landscape of UCP3 complex. We used the proteomic approach – affinity purification followed by mass spectrometry (AP-MS). Compared to the traditional approach such as yeast two-hybrid, mass spectrometry is more sensitive, time-efficient, quantitative and the is able to detect indirect protein-protein interaction.

Another goal of this investigation was to study the effect of UCP3 on genome-wide DNA methylation. Defective metabolism is one of the leading causes of uncontrolled epigenetic changes. Consequently, the UCP3 may have an indirect role in epigenetic regulation by maintaining normal mitochondrial respiration. Our hypothesis is that UCP3-deficient animals should show a significant difference in global methylation level compared to wild-type animal. And we conducted a pilot study to verify this hypothesis.

In summary, mitochondrial uncoupling proteins play a pivotal role in the regulation of mitochondrial respiration. Dysregulation of these proteins can cause an array of different disease states. Our study will contribute to the understanding of UCP3 function, and may provide certain insights in prevention and therapies for these UCP3-related diseases.

Chapter 2 methods and materials

2.1 Chemicals and Reagents

Unless otherwise stated, all reagents and chemicals were obtained from Sigma-Aldrich (St. Louis, MO).

2.2 Animals

C57BL/6J mice, C57BL/6J UCP3 -/- mice and C57BL/6J-hUCP3-α1actin-SKM-TG+/+ mice were maintained on standard laboratory chow and a 12 hour light/dark cycle at room temperature. All procedures were approved by the University of Texas Institutional Animal Care and Use Committee (IACUC).

2.3 Isolation of Muscle Tissues

Mice were sacrificed via CO_2 asphyxiation and cervical dislocation. In mass spectrometry experiment, tibialis anterior, gastrocnemius, soleus, biceps, triceps, and pectoralis muscles were dissected and placed in ice-cold mitochondrial isolation buffer #1(100mM KCl, 500mM Tris-HCl, 2mM EGTA, pH 7.4). In DNA methylation experiment, gastrocnemius and soleus were dissected and flash freezed in liquid nitrogen and stored at -80˚C until processing.

2.4 Isolation of Mitochondria

Mitochondria were isolated from muscle tissues. Tissues were finely minced in ice-cold mitochondrial isolation buffer #1 and centrifuged at 500g to remove the residual fat. Then tissues were re-suspended in 50ml complete mitochondrial

isolation buffer #2 (100mM KCl, 500mM Tris-HCl, 2mM EGTA, 1mM ATP, 5mM $MgCl_2$, 0.5% BSA, pH 7.4) then transferred to a 30mL glass teflon homogenizer. After 30 strokes, the homogenates were centrifuged at 500g then applied to a 70µm cell strainer to clear supernatant. The supernatant was then centrifuged at 10,500 x g for 10min to pellet the mitochondria. Once isolated, mitochondrial pellets were resuspended in 800ul Immunoprecipitation buffer (50mM Tris-HCL, pH 7.5, 150mM NaCl, 1% Triton X-100 and protease inhibitors) using Bead Mill for 10 minutes.

2.5 Quantification of Mitochondrial Protein Levels

Mitochondrial protein levels were measured using the BCA Protein Assay Kit according to manufacturer's instructions (Pierce, Rockford, IL).

2.6 Immunoprecipitation

Protein lysates were prepared in 600 µl of immunoprecipitation buffer. Samples were incubated with either 12µg of rabbit anti-UCP3 antibody at 4°C for 12 hours with rotation. Protein A/G Sepharose beads (60µL) were added to each sample and then rotated for 5 hours at 4°C. Beads were then burned in 35ul high-stringency protein gel loading buffer. Supernatant was collected and run on Bio-Rad precast gel.

2.7 Mass Spectrometry

The coomassie stained gel was submitted to The University of Texas at Austin ICMB Core Facility, where the LC-MS/MS was operated. The results were viewed via software Scaffold 3 developed by Proteome Software, Inc.

2.8 Isolation of Genomic DNA from Muscle Tissues

20-30mg of muscle tissues was used for each reaction. The genomic DNA was isolated using Wizard® Genomic DNA Purification Kit according to manufacturer's instruction (Promega).

2.9 Quantification of Global DNA Methylation Level

200ng of genomic DNA was used for each reaction. The DNA methylation level was quantified using Imprint® Methylated DNA Quantification kit (Sigma-Aldrich, St. Louis, MO).

2.10 Statistics

Statistical evaluation of the data was performed using the student's t-test with significance level $p<0.05$. For all histograms, data are presented as averages with error bars representing standard error of the mean (SEM) from at least 3 independent experiments. Single factor analysis of variance (ANOVA) was performed to determine the difference between the means of the three groups with significance level $p<0.05$.

Chapter 3 Identification of Proteins Interaction Partners of UCP3

3.1 Introduction

Mitochondrial uncoupling proteins (UCP) mediate the proton leak across the inner mitochondrial membrane and thereby control the efficiency of OXPHOS. Proton leak dissipates the mitochondrial membrane potential and uncouple proton motive force from ATP synthesis. To date, five UCPs(UCP1-5) have been identified in mammals with distinct expression pattern. The prototype UCP1, expressed in brown adipose tissue, has the well-established physiological role in mediating cold-induced thermogenesis in rodents and human neonates (Enerbäck et al., 1997). Relative to UCP1, the roles of UCP2-5 in metabolism are less clear.

UCP3 is primarily expressed in skeletal muscle, brown adipose tissue (BAT) and heart, all of which are highly metabolic and thermogenic tissues in humans (Boss et al., 1997; Gong et al., 1997). The expression level of UCP3 in skeletal muscle is relatively low - only 0.1%-1% as much as UCP1 in BAT. But considering the huge mass of skeletal muscle and its contribution to metabolic rate, UCP3 is still believed to play a pivotal role in metabolism.

UCP3 have been demonstrated to regulate the transport of fatty acid anions, protons and calcium across the inner mitochondrial membrane, and consequently mitigate ROS generation (Fedorenko et al., 2012). However, the biochemical mechanisms underlying UCP3-regulated solute transport and proton leak are intensely debated.

Several proteins have been identified to interact with UCP3 and facilitate different aspects of UCP3 functions. However, the identification of more interaction partners is necessary for further understanding the biochemical mechanism of

respiratory uncoupling and regulatory pathway of UCP3.

The traditional approach to study protein-protein interactions is yeast two-hybrid, which generally takes two to three months and has a high false-positive rate. Moreover, yeast two-hybrid is not able to detect indirect interaction between two proteins. Nowadays, the advent of the highly sensitive MS-based protein identification methods significantly enhances the efficiency of research. The availability of proteomic sequence database and the development of bioinformatics algorithm further automatize the protein identification process, allowing us to find the proteomic protein network easily and rapidly. Here, we used the proteomic approach – affinity purification followed by mass spectrometry, which gave us a comprehensive list of all mitochondrial proteins that potentially interact with UCP3. These target proteins can shed light on the future researches in defining novel mechanisms of UCP3.

3.2 Result

The complete list of proteins interacting with UCP3 is displayed in Table 3.1. All the peptide sequences are aligned with NCBI protein sequence databases and protein identity are accurate with probability >95%. The peak numbers represent how many times this specific protein has been identified, and hence semi-quantitatively though not accurately exhibit the amount of protein immune-precipitated along with UCP3.

In this list, we were able to observe a relatively high number of UCP3 peaks (42 peaks) in mitochondria isolated from UCP3 wild-type mice. This suggests the immune-precipitation experiment was able to successfully pull down detectable amount of UCP3. In contrast, there was no UCP3 peak identified in mitochondria of UCP3 knock-out mice (control group), which suggests the high peak number of UCP3 in wild-type mice is not due to contamination during the experiment.

We have successfully identified around 170 target proteins as direct or indirect

binding partner of UCP3. Among them, we are able to observe some proteins exhibiting significant difference between the experimental group and the control group, which are less possible to be false-positives due to non-specific protein-protein interaction. We set an arbitrary criterion: the proteins whose peak number is two-fold or higher in the wild-type group than the knock-out group are regarded as significantly different. These proteins will be discussed in the next section.

Table 3.1 The Complete List of Protein-Protein Interactions of UCP3

#	Identified Proteins (171)	Accession Number	Mol. Weight	Peak # In WT	Peak # in KO
1	Stress-70 protein, mitochondrial OS=Mus musculus GN=Hspa9 PE=1 SV=3	sp|P38647|GRP75_MOUSE	73 kDa	137	166
2	ATP synthase subunit alpha, mitochondrial OS=Mus musculus GN=Atp5a1 PE=1 SV=1	sp|Q03265|ATPA_MOUSE	60 kDa	149	73
3	ATP synthase subunit beta, mitochondrial OS=Mus musculus GN=Atp5b PE=1 SV=2	sp|P56480|ATPB_MOUSE	56 kDa	117	106
4	Sarcoplasmic/endoplasmic reticulum calcium ATPase 1 OS=Mus musculus GN=Atp2a1 PE=2 SV=1	sp|Q8R429|AT2A1_MOUSE	109 kDa	139	71
5	Rho guanine nucleotide exchange factor 10-like protein (Fragment) OS=Mus musculus GN=Arhgef10l PE=4 SV=1	tr|F6ZH54|F6ZH54_MOUSE-R	?	37	0
6	Aconitate hydratase, mitochondrial OS=Mus musculus GN=Aco2 PE=1 SV=1	sp|Q99KI0|ACON_MOUSE	85 kDa	82	22
7	ADP/ATP translocase 1 OS=Mus musculus GN=Slc25a4 PE=1 SV=4	sp|P48962|ADT1_MOUSE	33 kDa	50	29
8	Histone H1.2 OS=Mus musculus GN=Hist1h1c PE=1 SV=2	sp|P15864|H12_MOUSE	21 kDa	26	33

Table 3.1 The Complete List of Protein-Protein Interactions of UCP3 (Con't)

9	Isocitrate dehydrogenase 3 (NAD+) beta OS=Mus musculus GN=Idh3b PE=2 SV=1	tr|Q91VA7|Q91VA7_MOUSE	42 kDa	38	21
10	Dihydrolipoyllysine-residue acetyltransferase component of pyruvate dehydrogenase complex, mitochondrial OS=Mus musculus GN=Dlat PE=1 SV=2	sp|Q8BMF4|ODP2_MOUSE	68 kDa	29	25
11	Very long-chain specific acyl-CoA dehydrogenase, mitochondrial OS=Mus musculus GN=Acadvl PE=1 SV=3	sp|P50544|ACADV_MOUSE	71 kDa	45	8
12	Myosin-binding protein C, fast-type OS=Mus musculus GN=Mybpc2 PE=1 SV=1	sp|Q5XKE0|MYPC2_MOUSE	127 kDa	15	34
13	Mitochondrial uncoupling protein 3 OS=Mus musculus GN=Ucp3 PE=2 SV=1	sp|P56501|UCP3_MOUSE	34 kDa	42	0
14	78 kDa glucose-regulated protein OS=Mus musculus GN=Hspa5 PE=1 SV=3	sp|P20029|GRP78_MOUSE	72 kDa	16	25
15	Succinate dehydrogenase [ubiquinone] flavoprotein subunit, mitochondrial OS=Mus musculus GN=Sdha PE=1 SV=1	sp|Q8K2B3|DHSA_MOUSE	73 kDa	28	12
16	Calsequestrin-1 OS=Mus musculus GN=Casq1 PE=2 SV=3	sp|O09165|CASQ1_MOUSE	46 kDa	21	16

Table 3.1 The Complete List of Protein-Protein Interactions of UCP3 (Con't)

17	Heat shock cognate 71 kDa protein OS=Mus musculus GN=Hspa8 PE=1 SV=1	sp|P63017|HSP7C_MOUSE	71 kDa	9	28
18	Isocitrate dehydrogenase [NAD] subunit alpha, mitochondrial OS=Mus musculus GN=Idh3a PE=1 SV=1	sp|Q9D6R2|IDH3A_MOUSE	40 kDa	22	17
19	Pyruvate dehydrogenase E1 component subunit beta, mitochondrial OS=Mus musculus GN=Pdhb PE=1 SV=1	sp|Q9D051|ODPB_MOUSE	39 kDa	23	13
20	3-ketoacyl-CoA thiolase, mitochondrial OS=Mus musculus GN=Acaa2 PE=1 SV=3	sp|Q8BWT1|THIM_MOUSE	42 kDa	23	13
21	Isoform 2 of Keratin, type I cytoskeletal 10 OS=Mus musculus GN=Krt10	sp|P02535-2|K1C10_MOUSE (+3)	57 kDa	8	9
22	Succinate dehydrogenase [ubiquinone] iron-sulfur subunit, mitochondrial OS=Mus musculus GN=Sdhb PE=1 SV=1	sp|Q9CQA3|DHSB_MOUSE	32 kDa	12	17
23	Succinyl-CoA ligase [ADP-forming] subunit beta, mitochondrial OS=Mus musculus GN=Sucla2 PE=1 SV=2	sp|Q9Z2I9|SUCB1_MOUSE	50 kDa	28	4
24	Complement C1q subcomponent subunit A OS=Mus musculus GN=C1qa PE=1 SV=2	sp|P98086|C1QA_MOUSE	26 kDa	18	13
25	Myosin-4 OS=Mus musculus GN=Myh4 PE=1 SV=1	sp|Q5SX39|MYH4_MOUSE	223 kDa	30	3

Table 3.1 The Complete List of Protein-Protein Interactions of UCP3 (Con't)

26	Actin, alpha skeletal muscle OS=Mus musculus GN=Acta1 PE=1 SV=1	sp|P68134|ACTS_MOUSE	42 kDa	18	9
27	Electron transfer flavoprotein subunit alpha, mitochondrial OS=Mus musculus GN=Etfa PE=1 SV=2	sp|Q99LC5|ETFA_MOUSE	35 kDa	19	11
28	Trifunctional enzyme subunit alpha, mitochondrial OS=Mus musculus GN=Hadha PE=1 SV=1	sp|Q8BMS1|ECHA_MOUSE	83 kDa	21	4
29	Fibromodulin OS=Mus musculus GN=Fmod PE=2 SV=1	sp|P50608|FMOD_MOUSE	43 kDa	7	14
30	Isoform 2 of Sarcalumenin OS=Mus musculus GN=Srl	sp|Q7TQ48-2|SRCA_MOUSE (+1)	54 kDa	15	11
31	Elongation factor Tu, mitochondrial OS=Mus musculus GN=Tufm PE=1 SV=1	sp|Q8BFR5|EFTU_MOUSE (+1)	50 kDa	20	5
32	Myosin-binding protein H OS=Mus musculus GN=Mybph PE=1 SV=2	sp|P70402|MYBPH_MOUSE	53 kDa	4	15
33	Succinyl-CoA ligase [ADP/GDP-forming] subunit alpha, mitochondrial OS=Mus musculus GN=Suclg1 PE=1 SV=4	sp|Q9WUM5|SUCA_MOUSE	36 kDa	16	8
34	Complement C1q subcomponent subunit B OS=Mus musculus GN=C1qb PE=1 SV=2	sp|P14106|C1QB_MOUSE	27 kDa	10	12

Table 3.1 The Complete List of Protein-Protein Interactions of UCP3 (Con't)

35	Complement C1q subcomponent subunit C OS=Mus musculus GN=C1qc PE=2 SV=2	sp|Q02105|C1QC_MOUSE	26 kDa	11	9
36	Ryanodine receptor 1 OS=Mus musculus GN=Ryr1 PE=1 SV=1	sp|E9PZQ0|RYR1_MOUSE (+1)	565 kDa	16	5
37	Glyceraldehyde-3-phosphate dehydrogenase OS=Mus musculus GN=Gapdh PE=1 SV=2	sp|P16858|G3P_MOUSE	36 kDa	15	7
38	Pyruvate dehydrogenase E1 component subunit alpha, somatic form, mitochondrial OS=Mus musculus GN=Pdha1 PE=1 SV=1	sp|P35486|ODPA_MOUSE	43 kDa	10	10
39	Glycerol-3-phosphate dehydrogenase, mitochondrial OS=Mus musculus GN=Gpd2 PE=1 SV=2	sp|Q64521|GPDM_MOUSE (+1)	81 kDa	14	5
40	Keratin, type II cytoskeletal 8 OS=Mus musculus GN=Krt8 PE=1 SV=4	sp|P11679|K2C8_MOUSE	55 kDa	7	11
41	Myosin regulatory light chain 2, skeletal muscle isoform OS=Mus musculus GN=Mylpf PE=1 SV=3	sp|P97457|MLRS_MOUSE	19 kDa	8	9
42	Calcium-binding mitochondrial carrier protein Aralar1 OS=Mus musculus GN=Slc25a12 PE=1 SV=1	sp|Q8BH59|CMC1_MOUSE	75 kDa	14	4
43	Serum albumin OS=Mus musculus GN=Alb PE=1 SV=3	sp|P07724|ALBU_MOUSE	69 kDa	7	0

Table 3.1 The Complete List of Protein-Protein Interactions of UCP3 (Con't)

44	Isoform 2 of Ig gamma-2B chain C region OS=Mus musculus GN=Igh-3	sp|P01867-2|IGG2B_MOUSE (+1)	37 kDa	5	4
45	NADH dehydrogenase [ubiquinone] 1 alpha subcomplex subunit 4 OS=Mus musculus GN=Ndufa4 PE=1 SV=2	sp|Q62425|NDUA4_MOUSE	9 kDa	11	7
46	Tripartite motif-containing protein 72 OS=Mus musculus GN=Trim72 PE=1 SV=1	sp|Q1XH17|TRI72_MOUSE	53 kDa	13	3
47	Isoform 2 of 2-oxoglutarate dehydrogenase, mitochondrial OS=Mus musculus GN=Ogdh	sp|Q60597-2|ODO1_MOUSE (+3)	115 kDa	11	1
48	ATP synthase subunit O, mitochondrial OS=Mus musculus GN=Atp5o PE=1 SV=1	sp|Q9DB20|ATPO_MOUSE	23 kDa	15	0
49	Enoyl-CoA delta isomerase 1, mitochondrial OS=Mus musculus GN=Eci1 PE=2 SV=2	sp|P42125|ECI1_MOUSE	32 kDa	11	5
50	Titin OS=Mus musculus GN=Ttn PE=1 SV=1	sp|A2ASS6|TITIN_MOUSE-R	?	2	3
51	Creatine kinase S-type, mitochondrial OS=Mus musculus GN=Ckmt2 PE=1 SV=1	sp|Q6P8J7|KCRS_MOUSE	47 kDa	10	3

Table 3.1 The Complete List of Protein-Protein Interactions of UCP3 (Con't)

52	Isocitrate dehydrogenase [NAD] subunit gamma 1, mitochondrial OS=Mus musculus GN=Idh3g PE=1 SV=1	sp|P70404|IDHG1_MOUSE	43 kDa	9	3
53	Trifunctional enzyme subunit beta, mitochondrial OS=Mus musculus GN=Hadhb PE=1 SV=1	sp|Q99JY0|ECHB_MOUSE	51 kDa	12	0
54	Long-chain specific acyl-CoA dehydrogenase, mitochondrial OS=Mus musculus GN=Acadl PE=2 SV=2	sp|P51174|ACADL_MOUSE	48 kDa	6	5
55	Carnitine O-palmitoyltransferase 1, muscle isoform OS=Mus musculus GN=Cpt1b PE=2 SV=1	sp|Q924X2|CPT1B_MOUSE	88 kDa	11	0
56	Acetyl-CoA acetyltransferase, mitochondrial OS=Mus musculus GN=Acat1 PE=1 SV=1	sp|Q8QZT1|THIL_MOUSE	45 kDa	8	2
57	60 kDa heat shock protein, mitochondrial OS=Mus musculus GN=Hspd1 PE=1 SV=1	sp|P63038|CH60_MOUSE	61 kDa	6	0
58	Dihydrolipoyllysine-residue succinyltransferase component of 2-oxoglutarate dehydrogenase complex, mitochondrial OS=Mus musculus GN=Dlst PE=1 SV=1	sp|Q9D2G2|ODO2_MOUSE	49 kDa	5	4
59	Advanced glycosylation end product-specific receptor OS=Mus musculus GN=Ager PE=1 SV=1	sp|Q62151|RAGE_MOUSE (+4)	43 kDa	4	5
60	Dihydrolipoyl dehydrogenase, mitochondrial OS=Mus musculus GN=Dld PE=1 SV=2	sp|O08749|DLDH_MOUSE	54 kDa	9	0

Table 3.1 The Complete List of Protein-Protein Interactions of UCP3 (Con't)

61	Polyubiquitin-B OS=Mus musculus GN=Ubb PE=1 SV=1	sp|P0CG49|UBB_MOUSE (+9)	34 kDa	0	0
62	Ig kappa chain V-II region 26-10 OS=Mus musculus PE=1 SV=1	sp|P01631|KV2A7_MOUSE	12 kDa	0	5
63	Ig mu chain C region secreted form OS=Mus musculus GN=Igh-6 PE=1 SV=2	sp|P01872|IGHM_MOUSE (+1)	50 kDa	3	5
64	Pyruvate dehydrogenase protein X component, mitochondrial OS=Mus musculus GN=Pdhx PE=2 SV=1	sp|Q8BKZ9|ODPX_MOUSE	54 kDa	4	4
65	Complement C4-B OS=Mus musculus GN=C4b PE=1 SV=3	sp|P01029|CO4B_MOUSE	193 kDa	3	4
66	Myosin light chain 1/3, skeletal muscle isoform OS=Mus musculus GN=Myl1 PE=1 SV=2	sp|P05977|MYL1_MOUSE (+1)	21 kDa	6	0
67	ATP synthase gamma chain OS=Mus musculus GN=Atp5c1 PE=3 SV=1	tr|A2AKU9|A2AKU9_MOUSE	33 kDa	7	0
68	Histone H1.4 OS=Mus musculus GN=Hist1h1e PE=1 SV=2	sp|P43274|H14_MOUSE	22 kDa	4	0
69	Eukaryotic translation initiation factor 3 subunit C OS=Mus musculus GN=Eif3c PE=1 SV=1	sp|Q8R1B4|EIF3C_MOUSE-R	?	4	0

Table 3.1 The Complete List of Protein-Protein Interactions of UCP3 (Con't)

70	Junction plakoglobin OS=Mus musculus GN=Jup PE=1 SV=3	sp|Q02257|PLAK_MOUSE	82 kDa	3	4
71	Desmoplakin OS=Mus musculus GN=Dsp PE=3 SV=1	sp|E9Q557|DESP_MOUSE	333 kDa	5	3
72	Microtubule-actin cross-linking factor 1 OS=Mus musculus GN=Macf1 PE=1 SV=2	sp|Q9QXZ0|MACF1_MOUSE (+3)	832 kDa	0	2
73	Electron transfer flavoprotein subunit beta OS=Mus musculus GN=Etfb PE=1 SV=3	sp|Q9DCW4|ETFB_MOUSE	28 kDa	5	1
74	Beta-globin OS=Mus musculus GN=Hbb-b1 PE=3 SV=1	tr|A8DUK4|A8DUK4_MOUSE (+1)	16 kDa	7	0
75	Isoform 2 of Sacsin OS=Mus musculus GN=Sacs	sp|Q9JLC8-2|SACS_MOUSE-R (+3)	?	3	2
76	Malate dehydrogenase, mitochondrial OS=Mus musculus GN=Mdh2 PE=1 SV=3	sp|P08249|MDHM_MOUSE	36 kDa	5	0
77	AMP deaminase 1 OS=Mus musculus GN=Ampd1 PE=2 SV=1	sp|Q3V1D3|AMPD1_MOUSE (+2)	86 kDa	5	0

Table 3.1 The Complete List of Protein-Protein Interactions of UCP3 (Con't)

78	Structural maintenance of chromosomes flexible hinge domain-containing protein 1 OS=Mus musculus GN=Smchd1 PE=2 SV=2	sp|Q6P5D8|SMHD1_MOUSE	226 kDa	0	2
79	Nascent polypeptide-associated complex subunit alpha, muscle-specific form OS=Mus musculus GN=Naca PE=1 SV=2	sp|P70670|NACAM_MOUSE	220 kDa	2	2
80	Histone H2B type 1-F/J/L OS=Mus musculus GN=Hist1h2bf PE=1 SV=2	sp|P10853|H2B1F_MOUSE (+12)	14 kDa	4	0
81	Thioredoxin-dependent peroxide reductase, mitochondrial OS=Mus musculus GN=Prdx3 PE=1 SV=1	sp|P20108|PRDX3_MOUSE	28 kDa	4	0
82	Lipoamide acyltransferase component of branched-chain alpha-keto acid dehydrogenase complex, mitochondrial OS=Mus musculus GN=Dbt PE=2 SV=2	sp|P53395|ODB2_MOUSE	53 kDa	5	0
83	Glycine dehydrogenase [decarboxylating], mitochondrial OS=Mus musculus GN=Gldc PE=1 SV=1	sp|Q91W43|GCSP_MOUSE	113 kDa	0	3
84	Glycogen [starch] synthase, muscle OS=Mus musculus GN=Gys1 PE=1 SV=2	sp|Q9Z1E4|GYS1_MOUSE (+1)	84 kDa	5	0
85	Isocitrate dehydrogenase [NADP], mitochondrial OS=Mus musculus GN=Idh2 PE=1 SV=3	sp|P54071|IDHP_MOUSE	51 kDa	6	0

Table 3.1 The Complete List of Protein-Protein Interactions of UCP3 (Con't)

86	Kinectin OS=Mus musculus GN=Ktn1 PE=4 SV=1	tr|F8VQC7|F8VQC7_MOUSE-R	?	0	3
87	Isoform 2 of V-type proton ATPase catalytic subunit A OS=Mus musculus GN=Atp6v1a	sp|P50516-2|VATA_MOUSE (+2)	56 kDa	3	0
88	Ig gamma-2A chain C region secreted form OS=Mus musculus PE=1 SV=1	sp|P01864|GCAB_MOUSE (+1)	37 kDa	3	0
89	GrpE protein homolog 1, mitochondrial OS=Mus musculus GN=Grpel1 PE=1 SV=1	sp|Q99LP6|GRPE1_MOUSE	24 kDa	3	0
90	NADH dehydrogenase [ubiquinone] iron-sulfur protein 3, mitochondrial OS=Mus musculus GN=Ndufs3 PE=1 SV=2	sp|Q9DCT2|NDUS3_MOUSE	30 kDa	3	0
91	Glyceraldehyde-3-phosphate dehydrogenase OS=Mus musculus GN=Gm7251 PE=3 SV=1	tr|F6UT49|F6UT49_MOUSE	36 kDa	3	0
92	Isoform 2 of A-kinase anchor protein 10, mitochondrial OS=Mus musculus GN=Akap10	sp|O88845-2|AKA10_MOUSE-R	?	2	0
93	Uncharacterized protein OS=Mus musculus GN=Gm10073 PE=4 SV=1	tr|E9Q3T0|E9Q3T0_MOUSE	11 kDa	1	0
94	Granulins OS=Mus musculus GN=Grn PE=1 SV=2	sp|P28798|GRN_MOUSE (+1)	63 kDa	0	4

Table 3.1 The Complete List of Protein-Protein Interactions of UCP3 (Con't)

95	Protein capicua homolog OS=Mus musculus GN=Cic PE=1 SV=2	sp|Q924A2|CIC_MOUSE-R	?	0	2
96	Protein Spnb4 OS=Mus musculus GN=Spnb4 PE=4 SV=1	tr|E9PX29|E9PX29_MOUSE (+1)	289 kDa	2	0
97	Filamin-A OS=Mus musculus GN=Flna PE=1 SV=5	sp|Q8BTM8|FLNA_MOUSE (+2)	281 kDa	0	3
98	Isoform 2 of Probable helicase senataxin OS=Mus musculus GN=Setx	sp|A2AKX3-2|SETX_MOUSE (+1)	253 kDa	1	0
99	ADP/ATP translocase 2 OS=Mus musculus GN=Slc25a5 PE=1 SV=3	sp|P51881|ADT2_MOUSE	33 kDa	1	0
100	Aldehyde dehydrogenase, mitochondrial OS=Mus musculus GN=Aldh2 PE=1 SV=1	sp|P47738|ALDH2_MOUSE	57 kDa	4	0
101	Chaperone activity of bc1 complex-like, mitochondrial OS=Mus musculus GN=Adck3 PE=2 SV=2	sp|Q60936|ADCK3_MOUSE (+1)	72 kDa	5	0
102	Tropomodulin-3 OS=Mus musculus GN=Tmod3 PE=1 SV=1	sp|Q9JHJ0|TMOD3_MOUSE	40 kDa	0	0
103	MCG140437, isoform CRA_d OS=Mus musculus GN=Myh2 PE=4 SV=1	tr|G3UW82|G3UW82_MOUSE	223 kDa	4	0

Table 3.1 The Complete List of Protein-Protein Interactions of UCP3 (Con't)

104	Ig gamma-1 chain C region secreted form OS=Mus musculus GN=Ighg1 PE=1 SV=1	sp|P01868|IGHG1_MOUSE (+1)	36 kDa	0	5
105	ATP synthase subunit d, mitochondrial OS=Mus musculus GN=Atp5h PE=1 SV=3	sp|Q9DCX2|ATP5H_MOUSE (+1)	19 kDa	5	0
106	Ubiquitin-protein ligase E3A OS=Mus musculus GN=Ube3a PE=2 SV=1	sp|O08759|UBE3A_MOUSE (+1)	101 kDa	0	0
107	Protein Ceacam13 OS=Mus musculus GN=Ceacam13 PE=2 SV=1	tr|Q9DAT7|Q9DAT7_MOUSE-R (+1)	?	2	0
108	Isoform 2 of DnaJ homolog subfamily A member 3, mitochondrial OS=Mus musculus GN=Dnaja3	sp|Q99M87-2|DNJA3_MOUSE (+2)	49 kDa	2	0
109	Protein Ahnak OS=Mus musculus GN=Ahnak PE=4 SV=1	tr|E9Q616|E9Q616_MOUSE	604 kDa	1	0
110	Uncharacterized protein KIAA0825 homolog OS=Mus musculus PE=2 SV=3	sp|Q3UPC7|K0825_MOUSE-R	?	1	0
111	Myelin protein P0 OS=Mus musculus GN=Mpz PE=1 SV=1	sp|P27573|MYP0_MOUSE (+1)	28 kDa	0	3
112	Neurofilament heavy polypeptide OS=Mus musculus GN=Nefh PE=1 SV=3	sp|P19246|NFH_MOUSE	117 kDa	1	0

Table 3.1 The Complete List of Protein-Protein Interactions of UCP3 (Con't)

113	Isoform 2 of Titin OS=Mus musculus GN=Ttn	sp|A2ASS6-2|TITIN_MOUSE (+3)	2986 kDa	0	2
114	von Willebrand factor A domain-containing protein 8 OS=Mus musculus GN=Vwa8 PE=2 SV=2	sp|Q8CC88|VWA8_MOUSE	213 kDa	2	0
115	Thioredoxin domain-containing protein 11 OS=Mus musculus GN=Txndc11 PE=2 SV=1	sp|Q8K2W3|TXD11_MOUSE-R	?	0	2
116	Isoform Cytoplasmic of Fumarate hydratase, mitochondrial OS=Mus musculus GN=Fh	sp|P97807-2|FUMH_MOUSE (+1)	50 kDa	3	0
117	Retrovirus-related Pol polyprotein LINE-1 OS=Mus musculus GN=Pol PE=1 SV=2	sp|P11369|POL2_MOUSE-R	?	1	0
118	Glycogen phosphorylase, muscle form OS=Mus musculus GN=Pygm PE=1 SV=3	sp|Q9WUB3|PYGM_MOUSE (+1)	97 kDa	3	0
119	Unconventional myosin-Ia OS=Mus musculus GN=Myo1a PE=2 SV=2	sp|O88329|MYO1A_MOUSE-R	?	3	0
120	Medium-chain specific acyl-CoA dehydrogenase, mitochondrial OS=Mus musculus GN=Acadm PE=1 SV=1	sp|P45952|ACADM_MOUSE	46 kDa	3	0

Table 3.1 The Complete List of Protein-Protein Interactions of UCP3 (Con't)

121	Aspartate-beta-hydroxylase OS=Mus musculus GN=Asph PE=4 SV=1	tr|A2AL78|A2AL78_MOUSE	26 kDa	4	0
122	Enoyl-CoA hydratase, mitochondrial OS=Mus musculus GN=Echs1 PE=1 SV=1	sp|Q8BH95|ECHM_MOUSE	31 kDa	4	0
123	60S acidic ribosomal protein P0 OS=Mus musculus GN=Rplp0 PE=1 SV=3	sp|P14869|RLA0_MOUSE (+1)	34 kDa	3	0
124	Triosephosphate isomerase OS=Mus musculus GN=Tpi1 PE=3 SV=1	tr|H7BXC3|H7BXC3_MOUSE (+1)	18 kDa	4	0
125	Alpha globin 1 OS=Mus musculus GN=Hba-a1 PE=2 SV=1	tr|Q91VB8|Q91VB8_MOUSE	15 kDa	4	0
126	Tubulin alpha-1B chain OS=Mus musculus GN=Tuba1b PE=1 SV=2	sp|P05213|TBA1B_MOUSE (+1)	50 kDa	2	0
127	Isoform 2 of Tyrosine-protein kinase JAK3 OS=Mus musculus GN=Jak3	sp|Q62137-2|JAK3_MOUSE-R (+1)	?	2	0
128	Protein 4930407I10Rik OS=Mus musculus GN=4930407I10Rik PE=4 SV=2	tr|D3Z5T8|D3Z5T8_MOUSE	168 kDa	1	0

Table 3.1 The Complete List of Protein-Protein Interactions of UCP3 (Con't)

129	Isoform 2 of Obscurin OS=Mus musculus GN=Obscn	sp|A2AAJ9-2|OBSCN_MOUSE (+3)	780 kDa	0	1
130	Isoform 2 of General transcription factor 3C polypeptide 1 OS=Mus musculus GN=Gtf3c1	sp|Q8K284-2|TF3C1_MOUSE-R (+1)	?	0	1
131	Caspase recruitment domain-containing protein 10 OS=Mus musculus GN=Card10 PE=2 SV=1	sp|P58660|CAR10_MOUSE-R (+1)	?	1	0
132	Protein Pcdhb1 OS=Mus musculus GN=Pcdhb1 PE=2 SV=1	tr|Q91Y08|Q91Y08_MOUSE	91 kDa	1	0
133	Nesprin-2 OS=Mus musculus GN=Syne2 PE=1 SV=2	sp|Q6ZWQ0|SYNE2_MOUSE-R (+1)	?	0	1
134	[Pyruvate dehydrogenase [lipoamide]] kinase isozyme 4, mitochondrial OS=Mus musculus GN=Pdk4 PE=2 SV=1	sp|O70571|PDK4_MOUSE	47 kDa	3	0
135	Tropomyosin beta chain OS=Mus musculus GN=Tpm2 PE=1 SV=1	sp|P58774|TPM2_MOUSE (+1)	33 kDa	3	0
136	Tubulin beta-4B chain OS=Mus musculus GN=Tubb4b PE=1 SV=1	sp|P68372|TBB4B_MOUSE (+1)	50 kDa	3	0

Table 3.1 The Complete List of Protein-Protein Interactions of UCP3 (Con't)

137	Acyl-CoA dehydrogenase family member 9, mitochondrial OS=Mus musculus GN=Acad9 PE=2 SV=2	sp|Q8JZN5|ACAD9_MOUSE	69 kDa	0	3
138	Nuclear pore membrane glycoprotein 210 OS=Mus musculus GN=Nup210 PE=1 SV=2	sp|Q9QY81|PO210_MOUSE-R	?	3	0
139	Isoform 2 of YEATS domain-containing protein 2 OS=Mus musculus GN=Yeats2	sp|Q3TUF7-2|YETS2_MOUSE (+2)	137 kDa	0	2
140	Long-chain-fatty-acid--CoA ligase 1 OS=Mus musculus GN=Acsl1 PE=1 SV=2	sp|P41216|ACSL1_MOUSE (+1)	78 kDa	2	0
141	Isoform 2 of Protein PTHB1 OS=Mus musculus GN=Bbs9	sp|Q811G0-2|PTHB1_MOUSE (+1)	98 kDa	0	1
142	Valine--tRNA ligase, mitochondrial OS=Mus musculus GN=Vars2 PE=2 SV=2	sp|Q3U2A8|SYVM_MOUSE (+2)	118 kDa	0	0
143	Probable JmjC domain-containing histone demethylation protein 2C OS=Mus musculus GN=Jmjd1c PE=4 SV=1	tr|G3UZM1|G3UZM1_MOUSE	282 kDa	1	0
144	Novel protein containing fibronectin type 3 FN3 domains OS=Mus musculus GN=Fnd3c2 PE=4 SV=1	tr|A2AP83|A2AP83_MOUSE-R	?	0	1

Table 3.1 The Complete List of Protein-Protein Interactions of UCP3 (Con't)

145	Fumarylacetoacetate hydrolase domain-containing protein 2A OS=Mus musculus GN=Fahd2 PE=1 SV=1	sp|Q3TC72|FAHD2_MOUSE	35 kDa	2	0
146	Isoform 2 of Neuralized-like protein 4 OS=Mus musculus GN=Neurl4	sp|Q5NCX5-2|NEUL4_MOUSE (+3)	165 kDa	2	0
147	Hexaprenyldihydroxybenzoate methyltransferase, mitochondrial OS=Mus musculus GN=Coq3 PE=2 SV=1	sp|Q8BMS4|COQ3_MOUSE	41 kDa	2	0
148	Mitochondrial 2-oxoglutarate/malate carrier protein OS=Mus musculus GN=Slc25a11 PE=1 SV=3	sp|Q9CR62|M2OM_MOUSE (+1)	34 kDa	2	0
149	Protein Pcdhb12 OS=Mus musculus GN=Pcdhb12 PE=3 SV=1	tr|F6V243|F6V243_MOUSE	87 kDa	2	0
150	Semaphorin-3G OS=Mus musculus GN=Sema3g PE=2 SV=1	sp|Q4LFA9|SEM3G_MOUSE	87 kDa	2	0
151	Anthrax toxin receptor 2 OS=Mus musculus GN=Antxr2 PE=2 SV=1	sp|Q6DFX2|ANTR2_MOUSE-R	?	0	2
152	EH domain-containing protein 2 OS=Mus musculus GN=Ehd2 PE=1 SV=1	sp|Q8BH64|EHD2_MOUSE	61 kDa	1	0
153	Neuroligin-1 OS=Mus musculus GN=Nlgn1 PE=1 SV=2	sp|Q99K10|NLGN1_MOUSE	94 kDa	0	1

Table 3.1 The Complete List of Protein-Protein Interactions of UCP3 (Con't)

154	Isoform SERCA2A of Sarcoplasmic/endoplasmic reticulum calcium ATPase 2 OS=Mus musculus GN=Atp2a2	sp|O55143-2|AT2A2_MOUSE-R (+2)	?	1	0
155	Fibrous sheath-interacting protein 2 OS=Mus musculus GN=Fsip2 PE=1 SV=3	sp|A2ARZ3|FSIP2_MOUSE	785 kDa	1	0
156	Protein Col6a3 OS=Mus musculus GN=Col6a3 PE=4 SV=2	tr|E9PWQ3|E9PWQ3_MOUSE-R (+1)	?	1	0
157	Protein Kif14 OS=Mus musculus GN=Kif14 PE=3 SV=1	tr|E9Q3T3|E9Q3T3_MOUSE	181 kDa	1	0
158	Complement C3 OS=Mus musculus GN=C3 PE=1 SV=3	sp|P01027|CO3_MOUSE	186 kDa	1	0
159	Isoform 2 of Growth/differentiation factor 7 OS=Mus musculus GN=Gdf7	sp|P43029-2|GDF7_MOUSE (+1)	47 kDa	0	0
160	Isoform 2 of Zinc finger protein 541 OS=Mus musculus GN=Znf541	sp|Q0GGX2-2|ZN541_MOUSE (+1)	142 kDa	0	1

Table 3.1 The Complete List of Protein-Protein Interactions of UCP3 (Con't)

161	Isoform 2 of Kelch domain-containing protein 10 OS=Mus musculus GN=Klhdc10	sp|Q6PAR0-2|KLD10_MOUSE (+1)	45 kDa	0	1
162	Isoform 2 of Integrator complex subunit 6 OS=Mus musculus GN=Ints6	sp|Q6PCM2-2|INT6_MOUSE (+1)	99 kDa	0	0
163	Midasin OS=Mus musculus GN=Mdn1 PE=3 SV=1	tr|A2ANY6|A2ANY6_MOUSE (+1)	630 kDa	0	1
164	Arf-GAP with SH3 domain, ANK repeat and PH domain-containing protein 3 OS=Mus musculus GN=Asap3 PE=2 SV=1	sp|Q5U464|ASAP3_MOUSE	99 kDa	0	1
165	Coiled-coil domain-containing protein 66 OS=Mus musculus GN=Ccdc66 PE=1 SV=3	sp|Q6NS45|CCD66_MOUSE (+2)	107 kDa	1	0
166	Multidrug resistance protein 1B OS=Mus musculus GN=Abcb1b PE=1 SV=1	sp|P06795|MDR1B_MOUSE	141 kDa	0	1
167	Integrin alpha-L OS=Mus musculus GN=Itgal PE=3 SV=1	tr|D3Z627|D3Z627_MOUSE	133 kDa	1	0
168	Isoform 2 of Kinesin-like protein KIF20B OS=Mus musculus GN=Kif20b	sp|Q80WE4-2|KI20B_MOUSE-R (+3)	?	0	1

Table 3.1 The Complete List of Protein-Protein Interactions of UCP3 (Con't)

169	Protein Fat1 OS=Mus musculus GN=Fat1 PE=4 SV=1	tr|F2Z4A3|F2Z4A3_MOUSE-R	?	0	1
170	60S ribosomal protein L24 OS=Mus musculus GN=Rpl24 PE=4 SV=1	tr|G5E8B9|G5E8B9_MOUSE	119 kDa	1	0
171	Isoform 2 of Sodium/potassium/calcium exchanger 4 OS=Mus musculus GN=Slc24a4	sp|Q8CGQ8-2|NCKX4_MOUSE-R (+3)	?	1	0

3.3 Discussion

Mitochondrial uncoupling protein 3 is believed to dissipate proton gradient across the inner mitochondrial protein and release the energy as heat. However, it is now a consensus that the primary role of UCP3 is not thermogenesis. Several theories exist regarding the function of UCP3, and several proteins binding with it have been identified. As it is generally believed that interacting proteins should be coordinating or functionally related, the endeavor we took to identify the UCP3 interaction partners on a proteomic scale may reveal more functions of UCP3 and help explain the existing theories.

The proteins detected by the mass spectrometry can be grouped into several categories. These categories indicate the potential functions UCP3 may be involved in.

(1) TCA cycle associated proteins, including malate dehydrogenase, isocitrate dehydrogenase subunits, isoform 2 of 2-oxoglutarate dehydrogenase, acetyl-CoA acetyltransferase, pyruvate dehydrogenase E1 component subunit beta, aconitate hydratase etc. UCP3 has been shown to influence TCA cycle by accelerating the electron transport chain and consequently refilling the pool of cofactors NAD^+ and $FAD2^+$. However, these interactions of UCP3 with the TCA cycle participating proteins appear to implicate a more direct role of UCP3 in regulating the TCA cycle.

(2) Fatty acid oxidation and uptake related proteins, including long-chain specific acyl-CoA dehydrogenase, very long-chain specific acyl-CoA dehydrogenase, medium-chain specific acyl-CoA dehydrogenase, trifunctional enzyme subunits, enoyl-CoA delta isomerase 1, enoyl-CoA hydratase, carnitine O-palmitoyltransferase 1 etc. The enoyl-CoA hydratase, also known as $\Delta^{3,5}\Delta^{2,4}$dienoyl-CoA isomerase (DCI), has been previously demonstrated to interact with UCP3 and promote unsaturated fatty acid oxidation in a UCP3-dependent manner. Our data confirmed this interaction, and proposed more

possible mechanisms how UCP3 can regulate fatty acid metabolism. In addition, though UCP3 itself has been speculated to directly transport fatty acid back and forth across the inner mitochondrial membrane, its interaction with carnitine O-palmitoyltransferase 1 seems to imply a novel function in fatty acid uptake by controlling its carnitinization. Furthermore, these interactions may also involve the regulatory pathway of UCP3 itself. Though many experiments have confirmed the function of fatty acid to activate UCPs, little is known about how fatty acid in matrix is passed along to the UCPs on the inner membrane (Hagen and Lowell, 2000; Ježek, 1999; Skulachev, 1999; Žáčková et al., 2003). The protein bridging the gap between UCP3 and fatty acid may bind with UCP3 and be identified in this list.

(3) Calcium transport related proteins, including sarcoplasmic/endoplasmic reticulum calcium ATPase 1, ryanodine receptor 1, calcium-binding mitochondrial carrier protein Aralar1, etc. Previous studies have shown the UCP3 is essential for calcium import into the mitochondrial matrix, but the detailed mechanism is still not elucidated (Trenker et al., 2007). Among these proteins, ryanodine receptor 1 has been proposed to be the mitochondrial calcium channel in cardiac muscle (Csordás et al., 2012). Thus, the ryanodine receptor 1 is highly likely to coordinate with UCP3 and catalyze the import of calcium into mitochondria. Besides, the other proteins in this group may facilitate this process as well.

(4) ATP synthesis and transport-related proteins, including ATP synthase subunit O,d and alpha, ATP synthase gamma chain, ADP/ATP translocase 1, and Creatine kinase S-type. UCP3 was known to influence ATP synthesis by reducing proton gradient and diminishing the proton motive force which ATP synthase utilizes. However, these interactions seem to indicate a novel mechanism by which UCP3 balance ATP generation and export by coordinating with these proteins.

(5) ETC-related protein: Succinate dehydrogenase [ubiquinone] flavoprotein subunit. The only component of ETC that interacts with UCP3 at a detectable

level is complex II. ceUCP4, the UCP homolog in C.elegans, has been shown to regulate complex II-based respiration by mediating succinate import (Pfeiffer et al., 2011). It is likely that UCP3 use a similar mechanism to regulate mitochondrial respiration by affecting complex II function.

It is noteworthy that some of the reduced interaction levels in UCP3 knock-out mitochondria may also be explained by decreased expression level of that protein. For example, in the absence of UCP3, a compensatory decrease in ETC protein expression levels may occur to prevent the high membrane potential and ROS generation. Therefore, these putative interaction partners are still to be validated to confirm its physiological relevance.

To sum up, this study is the first time that the MS-based approach is used to investigate the component of UCP3 complex. The data we obtained will shed light on the mechanisms how UCP3 coordinate with different proteins and exhibit its proposed physiological roles.

Chapter 4 Uncoupling Protein 3 affect Global DNA methylation

4.1 Introduction

Since first discovered in early 1940s, epigenetics has been found to be associated with almost all cellular activities. Epigenetic processes can change gene expression and cell phenotype without changing the DNA sequences. Simply by modifying gene promoters or histones, transcription of a gene can be induced or inhibited in response to various signals. Proper function of epigenetics is essential for many cell functions, while dysregulation of epigenetics always leads to severe health conditions.

Epigenetics includes DNA methylation and histone modifications (phosphorylation, methylation, acetylation, ubiquitination, etc. Among them, DNA methylation is the most well-characterized epigenetic modifications. DNA methyltransferase (DNMT) can add a methyl group onto cytosine and produce 5-methylcytosine. The CpG island occurs five times more frequently in gene promoter regions and is the most common site for DNA methylation events in differentiated cells. When a gene needs to be suppressed, its CpG island in promoter region will be methylated and transcription will be inhibited. Conversely, the gene expression can be activated by demethylation of 5-methylcytosine catalyzed by DNA demethylase.

By far no existing evidence has shown UCP3 has an effect on DNA methylation level. However, many diseases that UCP3 opposes (including cancers and diabetes) are characterized by epigenetics-associated aberrant gene expression (Esteller, 2002, Ehrlich, 2002; Weinhold, 2006). As the presence of UCP3 can protect against these diseases, it should be able to maintain the normal epigenetic marks on genomic DNA. In addition, defective metabolism (especially the accumulation of ROS) is known as the leading contributor to the aberrant epigenetic changes. Considering the pivotal role UCP3 plays in regulating

respiratory efficiency and ROS scavenging, we hypothesized UCP3 has an indirect effect on regulating DNA methylation.

To test the effect of UCP3 on DNA methylation, we conducted a pivot study to measure the global DNA methylation level in the presence or absence of UCP3. We used the skeletal muscle tissues isolated from UCP3 wild-type mice, UCP3 knock-out mice and transgenic mice that modestly (3-5 fold) overexpress UCP3 in skeletal muscle. If the hypothesis is true, the global DNA methylation in UCP3 knock-out muscle tissue should be significantly different from UCP3 wild-type and UCP3 SKM transgenic mice. The experiment result will be shown in the next section.

4.2 Results

Our hypothesis that the absence of UCP3 can influence the global DNA methylation level significantly is confirmed by the ELISA-based approach. The experiment was repeated four times. Each time the result demonstrated a consistent tendency that UCP3 knock-out skeletal muscle tissues acquire hypermethylation in genomic DNA compared to UCP3 wild-type and transgenic tissues. According to the data, the UCP3 wild-type and knock-out genomic DNA have average global methylation levels that are 28% and 45% of the control DNA respectively. Since the fully methylated control DNA does not come from mouse, these percentages cannot represent the real DNA methylation level in UCP3 wild-type and knock-out skeletal muscle tissues. In this sense, the genomic DNA methylation levels of knock-out group and transgenic group are normalized to the wild-type control group, and figure 4.1 represent the fold change between the three groups. As shown by the figure, UCP3 knock-out mice have an average 1.5-fold higher genomic DNA methylation level compared to the wild-type controls (Figure 4.1). Single-factor ANOVA analysis also showed a statistically

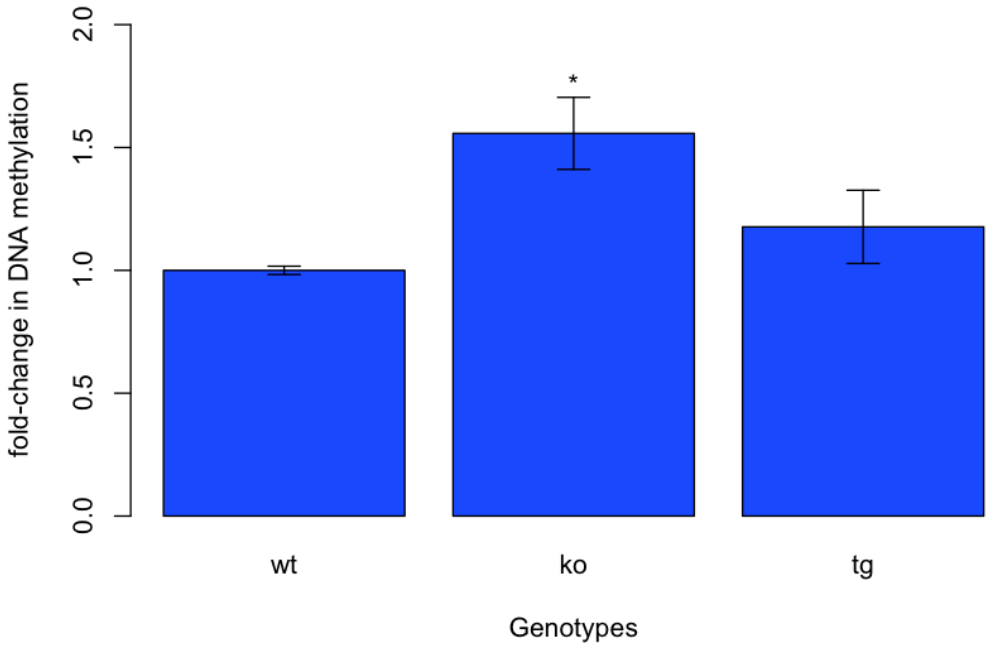

Figure 4.1 Genomic DNA isolated from UCP3 knock-out mice shows significantly induced global methylation level compared to UCP3 wild-type mice. The genomic DNA methylation level as expressed as fold-change relative to the wild-type control group. There is statistically significant difference between wild-type control group and UCP3 knock-out group. Assays were performed as described in the methods and materials. * indicate $p < 0.05$

significant difference between the wild-type control group and the knock-out group.

4.3 Discussion

Although it is well-established that metabolism plays a key role in the modulation of epigenetic processes, the relationship between uncoupling protein 3 and epigenetics has rarely been reported.

The prototypical UCPs (UCP1-3) are known for their ability to regulate proton conductance across the inner mitochondrial membrane and drive mitochondrial respiration. Consequently, UCP3 has been implicated in a number of metabolic functions, including ROS elimination and fatty acid transport. There are several putative mechanisms by which UCP3 can influence epigenetics: (1) By regulating the redox state in mitochondria, UCP3 may activate or inactivate DNMT and lead to DNA hypermethylation or hypomethylation respectively. (2) UCP3 can refuel the TCA cycle by liberating coenzyme A from fatty acid, which prevent the accumulation of TCA cycle metabolites. As succinate and fumarate have been shown to inhibit DNA demethylase, the normal function of TCA cycle is believed to be protective against abnormal epigenetic changes (Xiao et al., 2012).

We conducted the ELISA-based experiment to learn the effect of UCP3 on genomic DNA methylation levels. The result we observed supports our hypothesis that the absence of UCP3 will lead to a significant change in global DNA methylation level. Through this analysis we are able to establish a novel function of UCP3 in regulating the epigenetic processes in mammals. Additional experiments still need to be performed to investigate the detailed mechanism by which UCP3 regulate DNA methylation level.

Chapter 5 Concluding remarks and future directions

Since its discovery in 1997, there has been lots of controversy revolving the physiological or biochemical function of mitochondrial uncoupling protein 3 (UCP3). Just like UCP1, UCP3 is localized in the inner mitochondrial membrane and dissipate the proton gradient into the matrix. However, it was later demonstrated that UCP3 do not have the same function in maintaining body temperature as UCP1 (Vidal-Puig, Grujic et al. 2000). Though UCP3 has been related to promote thermogenesis in response to various stimuli, it is widely believed that UCP3 has more general roles in metabolism. UCP3 is primarily expressed in tissues with high metabolic rate, including heart, brown fat, and skeletal muscle (Vidal-Puig, Solanes et al. 1997). Given the huge mass of skeletal muscle, the UCP3-dependent mitochondrial uncoupling is speculated to have a significant role in the whole body metabolism.

Several mechanisms have been proposed as to the biochemical roles of UCP3. And some proteins that interact with UCP3 and facilitate its different functions have been identified and investigated. However, as more and more UCP3 interaction partners are discovered, we believe that UCP3 form a multi-protein complex, which may be involved in many different roles and be regulated by various signals. To validate our hypothesis, we performed a mass spectrometry-based analysis trying to identify the all components of UCP3 complex. More than 170 proteins were detected, most of which are related to at least one of the 5 following processes: TCA cycle, fatty acid metabolism and transport, calcium uptake, ATP synthesis and translocation, and electron transport chain. Though these protein-protein interactions with UCP3 are still to be confirmed by further experiment, these 5 groups will provide the directions for UCP3 study in the future.

The physiological roles of UCP3 have also been associated with the prevention of obesity, insulin resistance, type II diabetes and even cancer. Since all these

diseases are generally coupled with aberrant gene expression caused by epigenetic changes, the protective role of UCP3 may also include the maintenance of normal epigenetic marks. To answer this question, we conducted a pilot study on the effect of UCP3 deletion on DNA methylation level. The experiment result showed that UCP3 deficiency in animal muscle tissue contributes to genomic DNA hypermethylation, supporting the novel function of UCP3 in the maintenance of epigenetic processes. As the exact mechanism by which UCP3 regulate epigenetics are still unknown, further reports to explain the whole pathway are still needed. This model provides an explanation about how UCP3 can defend against the above-mentioned diseases, and may provide insights into the prevention and therapeutic strategies.

References

Barreiro, E., Garcia-Martínez, C., Mas, S., Ametller, E., Gea, J., Argilés, J.M., Busquets, S., and López-Soriano, F.J. (2009). UCP3 overexpression neutralizes oxidative stress rather than nitrosative stress in mouse myotubes. FEBS Lett. *583*, 350–356.

Barrès, R., Yan, J., Egan, B., Treebak, J.T., Rasmussen, M., Fritz, T., Caidahl, K., Krook, A., O'Gorman, D.J., and Zierath, J.R. (2012). Acute Exercise Remodels Promoter Methylation in Human Skeletal Muscle. Cell Metab. *15*, 405–411.

Bezaire, V., Spriet, L.L., Campbell, S., Sabet, N., Gerrits, M., Bonen, A., and Harper, M.-E. (2005). Constitutive UCP3 overexpression at physiological levels increases mouse skeletal muscle capacity for fatty acid transport and oxidation. FASEB J.

Bézaire, V., Seifert, E.L., and Harper, M.-E. (2007). Uncoupling protein-3: clues in an ongoing mitochondrial mystery. FASEB J. *21*, 312–324.

Boss, O., Samec, S., Paoloni-Giacobino, A., Rossier, C., Dulloo, A., Seydoux, J., Muzzin, P., and Giacobino, J.-P. (1997). Uncoupling protein-3: a new member of the mitochondrial carrier family with tissue-specific expression. FEBS Lett. *408*, 39–42.

Boss, O., Samec, S., Kühne, F., Bijlenga, P., Assimacopoulos-Jeannet, F., Seydoux, J., Giacobino, J.-P., and Muzzin, P. (1998). Uncoupling Protein-3 Expression in Rodent Skeletal Muscle Is Modulated by Food Intake but Not by Changes in Environmental Temperature. J. Biol. Chem. *273*, 5–8.

Bouillaud, F., Ricquier, D., Thibault, J., and Weissenbach, J. (1985). Molecular approach to thermogenesis in brown adipose tissue: cDNA cloning of the mitochondrial uncoupling protein. Proc. Natl. Acad. Sci. U. S. A. *82*, 445–448.

Boyer, P.D. (1997). The Atp Synthase—a Splendid Molecular Machine. Annu. Rev. Biochem. *66*, 717–749.

Brand, M.D., and Esteves, T.C. (2005). Physiological functions of the mitochondrial uncoupling proteins UCP2 and UCP3. Cell Metab. *2*, 85–93.

Cannon, B., and Nedergaard, J. (2004). Brown Adipose Tissue: Function and Physiological Significance. Physiol. Rev. *84*, 277–359.

Cannon, B., Hedin, A., and Nedergaard, J. (1982). Exclusive occurrence of thermogenin antigen in brown adipose tissue. FEBS Lett. *150*, 129–132.

Cedar, H., and Bergman, Y. (2009). Linking DNA methylation and histone modification: patterns and paradigms. Nat. Rev. Genet. *10*, 295–304.

Cervera, A.M., Bayley, J.-P., Devilee, P., and McCreath, K.J. (2009). Inhibition of succinate dehydrogenase dysregulates histone modification in mammalian cells. Mol. Cancer *8*, 89.

Chan, C.B., and Harper, M.-E. (2006). Uncoupling Proteins: Role in Insulin Resistance and Insulin Insufficiency. Curr. Diabetes Rev. *2*, 271–283.

Chan, C.B., MacDonald, P.E., Saleh, M.C., Johns, D.C., Marbàn, E., and Wheeler, M.B. (1999). Overexpression of uncoupling protein 2 inhibits glucose-stimulated insulin secretion from rat islets. Diabetes *48*, 1482–1486.

Chan, C.B., Leo, D.D., Joseph, J.W., McQuaid, T.S., Ha, X.F., Xu, F., Tsushima, R.G., Pennefather, P.S., Salapatek, A.M.F., and Wheeler, M.B. (2001). Increased Uncoupling Protein-2 Levels in β-cells Are Associated With Impaired Glucose-Stimulated Insulin Secretion Mechanism of Action. Diabetes *50*, 1302–1310.

Chowdhury, R., Yeoh, K.K., Tian, Y.-M., Hillringhaus, L., Bagg, E.A., Rose, N.R., Leung, I.K.H., Li, X.S., Woon, E.C.Y., Yang, M., et al. (2011). The oncometabolite 2- hydroxyglutarate inhibits histone lysine demethylases. EMBO Rep. *12*, 463–469.

Clapham JC, Arch JR, Chapman H, Haynes A, Lister C, Moore GB, Piercy V, Carter SA, Lehner I, Smith SA, Beeley LJ, Godden RJ, Herrity N, Skehel M, Changani KK, Hockings PD, Reid DG, Squires SM, Hatcher J, Trail B, Latcham J, Rastan S, Harper AJ, Cadenas S, Buckingham JA, Brand MD, Abuin A.(2000). Mice overexpressing human uncoupling protein-3 in skeletal muscle are hyperphagic and lean : Article : Nature. Nature *406*, 415–418.

Coppola, A., Liu, Z.-W., Andrews, Z.B., Paradis, E., Roy, M.-C., Friedman, J.M., Ricquier, D., Richard, D., Horvath, T.L., Gao, X.-B., et al. (2007). A Central Thermogenic-like Mechanism in Feeding Regulation: An Interplay between Arcuate Nucleus T3 and UCP2. Cell Metab. *5*, 21–33.

Csordás, G., Várnai, P., Golenár, T., Sheu, S.-S., and Hajnóczky, G. (2012). Calcium transport across the inner mitochondrial membrane: Molecular mechanisms and pharmacology. Mol. Cell. Endocrinol. *353*, 109–113.

Donkena, K.V., Young, C.Y.F., and Tindall, D.J. (2010). Oxidative Stress and DNA Methylation in Prostate Cancer. Obstet. Gynecol. Int. *2010*, e302051.

Echtay, K.S., Roussel, D., St-Pierre, J., Jekabsons, M.B., Cadenas, S., Stuart, J.A., Harper, J.A., Roebuck, S.J., Morrison, A., Pickering, S., et al. (2002). Superoxide activates mitochondrial uncoupling proteins. Nature *415*, 96–99.

Echtay, K.S., Esteves, T.C., Pakay, J.L., Jekabsons, M.B., Lambert, A.J., Portero-Otin, M., Pamplona, R., Vidal-Puig, A.J., Wang, S., Roebuck, S.J., et al. (2003). A signalling role for 4-hydroxy-2-nonenal in regulation of mitochondrial uncoupling. EMBO J. *22*, 4103–4110.

Enerbäck, S., Jacobsson, A., Simpson, E.M., Guerra, C., Yamashita, H., Harper, M.-E., and Kozak, L.P. (1997). Mice lacking mitochondrial uncoupling protein are cold-sensitive but not obese. Nature *387*, 90–94.

Enrlich, M. (2002). DNA methylation in cancer: too much, but also too little. Publ. Online 05 August 2002 Doi101038sjonc1205651 *21*.

Estellar, M. (2002). CpG island hypermethylation and tumor suppressor genes: a booming present, a brighter future. Publ. Online 05 August 2002 Doi101038sjonc1205600 *21*.

Esteves, T.C., and Brand, M.D. (2005). The reactions catalysed by the mitochondrial uncoupling proteins UCP2 and UCP3. Biochim. Biophys. Acta BBA - Bioenerg. *1709*, 35–44.

Fedorenko, A., Lishko, P.V., and Kirichok, Y. (2012). Mechanism of Fatty-Acid-Dependent UCP1 Uncoupling in Brown Fat Mitochondria. Cell *151*, 400–413.

Feldmann, H.M., Golozoubova, V., Cannon, B., and Nedergaard, J. (2009). UCP1 Ablation Induces Obesity and Abolishes Diet-Induced Thermogenesis in Mice Exempt from Thermal Stress by Living at Thermoneutrality. Cell Metab. *9*, 203–209.

Figueroa, M.E., Abdel-Wahab, O., Lu, C., Ward, P.S., Patel, J., Shih, A., Li, Y., Bhagwat, N., Vasanthakumar, A., Fernandez, H.F., et al. (2010). Leukemic IDH1 and IDH2 Mutations Result in a Hypermethylation Phenotype, Disrupt TET2 Function, and Impair Hematopoietic Differentiation. Cancer Cell *18*, 553–567.

Fleury, C., Neverova, M., Collins, S., Raimbault, S., Champigny, O., Levi-Meyrueis, C., Bouillaud, F., Seldin, M.F., Surwit, R.S., Ricquier, D., et al. (1997). Uncoupling protein-2: a novel gene linked to obesity and hyperinsulinemia. Nat. Genet. *15*, 269–272.

Garlid, K.D., Jabůrek, M., and Ježek, P. (1998). The mechanism of proton transport mediated by mitochondrial uncoupling proteins. FEBS Lett. *438*, 10–14.

Golozoubova, V., Hohtola, E., Matthias, A., Jacobsson, A., Cannon, B., and Nedergaard, J. (2001). Only UCP1 can mediate adaptive nonshivering thermogenesis in the cold. FASEB J.

Gong, D.-W., He, Y., Karas, M., and Reitman, M. (1997). Uncoupling Protein-3 Is a Mediator of Thermogenesis Regulated by Thyroid Hormone, β3-Adrenergic Agonists, and Leptin. J. Biol. Chem. *272*, 24129–24132.

Graier, W.F., Trenker, M., and Malli, R. (2008). Mitochondrial Ca2+, the secret behind the function of uncoupling proteins 2 and 3? Cell Calcium *44*, 36–50.

Hagen, T., and Lowell, B.B. (2000). Chimeric Proteins between UCP1 and UCP3: The Middle Third of UCP1 Is Necessary and Sufficient for Activation by Fatty Acids. Biochem. Biophys. Res. Commun. *276*, 642–648.

He, J., Xu, Q., Jing, Y., Agani, F., Qian, X., Carpenter, R., Li, Q., Wang, X.-R., Peiper, S.S., Lu, Z., et al. (2012). Reactive oxygen species regulate ERBB2 and ERBB3 expression via miR- 199a/125b and DNA methylation. EMBO Rep. *13*, 1116–1122.

Himms-Hagen, J., and Harper, M.-E. (2001). Physiological Role of UCP3 May Be Export of Fatty Acids from Mitochondria When Fatty Acid Oxidation Predominates: An Hypothesis. Exp. Biol. Med. *226*, 78–84.

Hirasaka, K., Lago, C.U., Kenaston, M.A., Fathe, K., Nowinski, S.M., Nikawa, T., and Mills, E.M. (2011). Identification of a Redox-Modulatory Interaction Between Uncoupling Protein 3 and Thioredoxin 2 in the Mitochondrial Intermembrane Space. Antioxid. Redox Signal. *15*, 2645–2661.

Hitchler, M.J., and Domann, F.E. (2009). Metabolic defects provide a spark for the epigenetic switch in cancer. Free Radic. Biol. Med. *47*, 115–127.

Hittelman, K.J., Lindberg, O., and Cannon, B. (1969). Oxidative Phosphorylation and Compartmentation of Fatty Acid Metabolism in Brown Fat Mitochondria. Eur. J. Biochem. *11*, 183–192.

Hood, D.A. (2009). Mechanisms of exercise-induced mitochondrial biogenesis in skeletal muscleThis paper is one of a selection of papers published in this Special Issue, entitled 14th International Biochemistry of Exercise Conference – Muscles as Molecular and Metabolic Machines, and has undergone the Journal's usual peer review process. Appl. Physiol. Nutr. Metab. *34*, 465–472.

Huang, S.-G. (2003). Limited proteolysis reveals conformational changes in uncoupling protein-1 from brown adipose tissue mitochondria. Arch. Biochem. Biophys. *420*, 40–45.

Iser, W.B., Kim, D., Bachman, E., and Wolkow, C. (2005). Examination of the requirement for ucp-4, a putative homolog of mammalian uncoupling proteins, for stress tolerance and longevity in C. elegans. Mech. Ageing Dev. *126*, 1090–1096.

Ivanova, M.V., Hoang, T., McSorley, F.R., Krnac, G., Smith, M.D., and Jelokhani-Niaraki, M. (2010). A Comparative Study on Conformation and Ligand Binding of the Neuronal Uncoupling Proteins. Biochemistry (Mosc.) *49*, 512–521.

Jabůrek, M., and Garlid, K.D. (2003). Reconstitution of Recombinant Uncoupling Proteins UCP1, -2, AND -3 HAVE SIMILAR AFFINITIES FOR ATP AND ARE UNAFFECTED BY COENZYME Q10. J. Biol. Chem. *278*, 25825–25831.

Ježek, P. (1999). Fatty Acid Interaction with Mitochondrial Uncoupling Proteins. J. Bioenerg. Biomembr. *31*, 457–466.

Ježek, P., Costa, A.D.T., and Vercesi, A.E. (1996). Evidence for Anion-translocating Plant Uncoupling Mitochondrial Protein in Potato Mitochondria. J. Biol. Chem. *271*, 32743–32748.

Ježek, P., Modrianský, M., and Garlid, K.D. (1997). A structure–activity study of fatty acid interaction with mitochondrial uncoupling protein. FEBS Lett. *408*, 166–170.

Ježek, P., Engstová, H., Žáčková, M., Vercesi, A.E., Costa, A.D.T., Arruda, P., and Garlid, K.D. (1998). Fatty acid cycling mechanism and mitochondrial uncoupling proteins. Biochim. Biophys. Acta BBA - Bioenerg. *1365*, 319–327.

Kang, K.A., Zhang, R., Kim, G.Y., Bae, S.C., and Hyun, J.W. (2012). Epigenetic changes induced by oxidative stress in colorectal cancer cells: methylation of tumor suppressor RUNX3. Tumor Biol. *33*, 403–412.

Kim-Han, J.S., Reichert, S.A., Quick, K.L., and Dugan, L.L. (2001). BMCP1: a mitochondrial uncoupling protein in neurons which regulates mitochondrial function and oxidant production. J. Neurochem. *79*, 658–668.

Klaus, S., Seivert, A., and Boeuf, S. (2001). Effect of the β3-adrenergic agonist Cl316,243 on functional differentiation of white and brown adipocytes in primary cell culture. Biochim. Biophys. Acta BBA - Mol. Cell Res. *1539*, 85–92.

Klingenberg, M., and Huang, S.-G. (1999). Structure and function of the uncoupling protein from brown adipose tissue. Biochim. Biophys. Acta BBA - Biomembr. *1415*, 271–296.

Korshunov, S.S., Skulachev, V.P., and Starkov, A.A. (1997). High protonic potential actuates a mechanism of production of reactive oxygen species in mitochondria. FEBS Lett. *416*, 15–18.

Krauss, S., Zhang, C.-Y., and Lowell, B.B. (2005). The mitochondrial uncoupling-protein homologues. Nat. Rev. Mol. Cell Biol. *6*, 248–261.

Lago, C., Nowinski, S., Rundhaug, J., Pfeiffer, M., Kiguchi, K., Hirasaka, K., Yang, X., Abramson, E., Bratton, S., Rho, O., et al. (2012). Mitochondrial respiratory uncoupling promotes keratinocyte differentiation and blocks skin carcinogenesis. Oncogene *31*, 4725–4731.

Laloi, M., Klein, M., Riesmeier, J.W., Müller-Röber, B., Fleury, C., Bouillaud, F., and Ricquier, D. (1997). A plant cold-induced uncoupling protein. Nature *389*, 135–136.

Larkin, S., Mull, E., Miao, W., Pittner, R., Albrandt, K., Moore, C., Young, A., Denaro, M., and Beaumont, K. (1997). Regulation of the Third Member of the Uncoupling Protein Family, UCP3, by Cold and Thyroid Hormone. Biochem. Biophys. Res. Commun. *240*, 222–227.

Li, E. (2002). Chromatin modification and epigenetic reprogramming in mammalian development. Nat. Rev. Genet. *3*, 662–673.

Li, L.-C., Carroll, P.R., and Dahiya, R. (2005). Epigenetic Changes in Prostate Cancer: Implication for Diagnosis and Treatment. J. Natl. Cancer Inst. *97*, 103–115.

Li, L.-X., Skorpen, F., Egeberg, K., Jørgensen, I.H., and Grill, V. (2001). Uncoupling Protein-2 Participates in Cellular Defense against Oxidative Stress in Clonal β-Cells. Biochem. Biophys. Res. Commun. *282*, 273–277.

Li, Y., Maedler, K., Shu, L., and Haataja, L. (2008). UCP-2 and UCP-3 Proteins Are Differentially Regulated in Pancreatic Beta-Cells. PLoS ONE *3*, e1397.

Lim, S.-O., Gu, J.-M., Kim, M.S., Kim, H.-S., Park, Y.N., Park, C.K., Cho, J.W., Park, Y.M., and Jung, G. (2008). Epigenetic Changes Induced by Reactive Oxygen Species in Hepatocellular Carcinoma: Methylation of the E-cadherin Promoter. Gastroenterology *135*, 2128–2140.e8.

Liu, D., Chan, S.L., Souza-Pinto, N.C. de, Jr, J.R.S., Wersto, R.P., Zhan, M., Mustafa, K., Cabo, R. de, and Mattson, M.P. (2006). Mitochondrial UCP4 mediates an adaptive shift in energy metabolism and increases the resistance of neurons to metabolic and oxidative stress. NeuroMolecular Med. *8*, 389–413.

Maloney, P.C. (1990). A consensus structure for membrane transport. Res. Microbiol. *141*, 374–395.

Mao, W., Yu, X.X., Zhong, A., Li, W., Brush, J., Sherwood, S.W., Adams, S.H., and Pan, G. (1999). UCP4, a novel brain-specific mitochondrial protein that reduces membrane potential in mammalian cells. FEBS Lett. *443*, 326–330.

Matthias, A., Ohlson, K.B.E., Fredriksson, J.M., Jacobsson, A., Nedergaard, J., and Cannon, B. (2000). Thermogenic Responses in Brown Fat Cells Are Fully UCP1-dependent UCP2 OR UCP3 DO NOT SUBSTITUTE FOR UCP1 IN ADRENERGICALLY OR FATTY ACID-INDUCED THERMOGENESIS. J. Biol. Chem. *275*, 25073–25081.

Mattiasson, G., and Sullivan, P.G. (2006). The Emerging Functions of UCP2 in Health, Disease, and Therapeutics. Antioxid. Redox Signal. *8*, 1–38.

Mattson, M.P., and Liu, D. (2003). Mitochondrial potassium channels and uncoupling proteins in synaptic plasticity and neuronal cell death. Biochem. Biophys. Res. Commun. *304*, 539–549.

Mills, E.M., Banks, M.L., Sprague, J.E., and Finkel, T. (2003). Pharmacology: Uncoupling the agony from ecstasy. Nature *426*, 403–404.

Moreno-Sánchez, R., Rodríguez-Enríquez, S., Marín-Hernández, A., and Saavedra, E. (2007). Energy metabolism in tumor cells. FEBS J. *274*, 1393–1418.

Mori, S., Yoshizuka, N., Takizawa, M., Takema, Y., Murase, T., Tokimitsu, I., and Saito, M. (2008). Expression of Uncoupling Proteins in Human Skin and Skin-Derived Cells. J. Invest. Dermatol. *128*, 1894–1900.

Naviaux, R.K. (2008). Mitochondrial control of epigenetics. Cancer Biol. Ther. *7*, 1191–1193.

Nedergaard, J., Bengtsson, T., and Cannon, B. (2007). Unexpected evidence for active brown adipose tissue in adult humans. Am. J. Physiol. - Endocrinol. Metab. *293*, E444–E452.

Nicholls, D.G. (1976). Hamster Brown-Adipose-Tissue Mitochondria. Eur. J. Biochem. *62*, 223–228.

Nicholls, D.G. (2006). The physiological regulation of uncoupling proteins. Biochim. Biophys. Acta BBA - Bioenerg. *1757*, 459–466.

Palmieri, F. (2004). The mitochondrial transporter family (SLC25): physiological and pathological implications. Pflüg. Arch. *447*, 689–709.

Parker, N., Vidal-Puig, A., and Brand, M.D. (2008). Stimulation of mitochondrial proton conductance by hydroxynonenal requires a high membrane potential. Biosci. Rep. *28*, 83–88.

Parker, N., Crichton, P.G., Vidal-Puig, A.J., and Brand, M.D. (2009). Uncoupling protein-1 (UCP1) contributes to the basal proton conductance of brown adipose tissue mitochondria. J. Bioenerg. Biomembr. *41*, 335–342.

Pfeiffer, M., Kayzer, E.-B., Yang, X., Abramson, E., Kenaston, M.A., Lago, C.U., Lo, H.-H., Sedensky, M.M., Lunceford, A., Clarke, C.F., et al. (2011). Caenorhabditis elegans UCP4 Protein Controls Complex II-mediated Oxidative Phosphorylation through Succinate Transport. J. Biol. Chem. *286*, 37712–37720.

Porter, R.K. (2008). Uncoupling protein 1: a short-circuit in the chemiosmotic process. J. Bioenerg. Biomembr. *40*, 457–461.

Quan, X., Lim, S.-O., and Jung, G. (2011). Reactive oxygen species downregulate catalase expression via methylation of a CpG Island in the Oct-1 promoter. FEBS Lett. *585*, 3436–3441.

Robinson, A.J., Overy, C., and Kunji, E.R.S. (2008). The mechanism of transport by mitochondrial carriers based on analysis of symmetry. Proc. Natl. Acad. Sci. *105*, 17766–17771.

Rodríguez-Cuenca, S., Pujol, E., Justo, R., Frontera, M., Oliver, J., Gianotti, M., and Roca, P. (2002). Sex-dependent Thermogenesis, Differences in Mitochondrial Morphology and Function, and Adrenergic Response in Brown Adipose Tissue. J. Biol. Chem. *277*, 42958–42963.

Rolfe, D.F.S., Newman, J.M.B., Buckingham, J.A., Clark, M.G., and Brand, M.D. (1999). Contribution of mitochondrial proton leak to respiration rate in working skeletal muscle and liver and to SMR. Am. J. Physiol. - Cell Physiol. *276*, C692–C699.

Rottenberg, H. (1975). The measurement of transmembrane electrochemical proton gradients. J. Bioenerg. *7*, 61–74.

Rutter, G.A. (2001). Nutrient–secretion coupling in the pancreatic islet β-cell: recent advances. Mol. Aspects Med. *22*, 247–284.

Sanchez-Blanco, A., Fridell, Y.-W.C., and Helfand, S.L. (2006). Involvement of Drosophila Uncoupling Protein 5 in Metabolism and Aging. Genetics *172*, 1699–1710.

Sanchis, D., Fleury, C., Chomiki, N., Goubern, M., Huang, Q., Neverova, M., Grégoire, F., Easlick, J., Raimbault, S., Lévi-Meyrueis, C., et al. (1998). BMCP1, a Novel Mitochondrial Carrier with High Expression in the Central Nervous System of Humans and Rodents, and Respiration Uncoupling Activity in Recombinant Yeast. J. Biol. Chem. *273*, 34611–34615.

Schrauwen, P., Saris, W.H.M., and Hesselink, M.K.C. (2001). An alternative function for human uncoupling protein 3: protection of mitochondria against accumulation of nonesterified fatty acids inside the mitochondrial matrix. FASEB J. *15*, 2497–2502.

Schrauwen, P., Hoeks, J., and Hesselink, M.K.C. (2006). Putative function and physiological relevance of the mitochondrial uncoupling protein-3: Involvement in fatty acid metabolism? Prog. Lipid Res. *45*, 17–41.

Schultz, B.E., and Chan, S.I. (2001). Structures and Proton-Pumping Strategies of Mitochondrial Respiratory Enzymes. Annu. Rev. Biophys. Biomol. Struct. *30*, 23–65.

Skulachev, V.P. (1999). Anion Carriers in Fatty Acid-Mediated Physiological Uncoupling. J. Bioenerg. Biomembr. *31*, 431–445.

Smith, R.E., and Horwitz, B.A. (1969). Brown fat and thermogenesis. Physiol. Rev. *49*, 330–425.

Smorodchenko, A., Rupprecht, A., Sarilova, I., Ninnemann, O., Bräuer, A.U., Franke, K., Schumacher, S., Techritz, S., Nitsch, R., Schuelke, M., et al. (2009). Comparative analysis of uncoupling protein 4 distribution in various tissues under physiological conditions and during development. Biochim. Biophys. Acta BBA - Biomembr. *1788*, 2309–2319.

Stuart, J.A., Harper, J.A., Brindle, K.M., and Brand, M.D. (1999). Uncoupling protein 2 from carp and zebrafish, ectothermic vertebrates. Biochim. Biophys. Acta BBA - Bioenerg. *1413*, 50–54.

Talbot, D.A., Hanuise, N., Rey, B., Rouanet, J.-L., Duchamp, C., and Brand, M.D. (2003). Superoxide activates a GDP-sensitive proton conductance in skeletal muscle mitochondria from king penguin (Aptenodytes patagonicus). Biochem. Biophys. Res. Commun. *312*, 983–988.

Talbot, D.A., Lambert, A.J., and Brand, M.D. (2004). Production of endogenous matrix superoxide from mitochondrial complex I leads to activation of uncoupling protein 3. FEBS Lett. *556*, 111–115.

Tateishi, K., Okada, Y., Kallin, E.M., and Zhang, Y. (2009). Role of Jhdm2a in regulating metabolic gene expression and obesity resistance. Nature *458*, 757–761.

Trenker, M., Malli, R., Fertschai, I., Levak-Frank, S., and Graier, W.F. (2007). Uncoupling proteins 2 and 3 are fundamental for mitochondrial Ca2+ uniport. Nat. Cell Biol. *9*, 445–452.

Turcan, S., Rohle, D., Goenka, A., Walsh, L.A., Fang, F., Yilmaz, E., Campos, C., Fabius, A.W.M., Lu, C., Ward, P.S., et al. (2012). IDH1 mutation is sufficient to establish the glioma hypermethylator phenotype. Nature *483*, 479–483.

Vidal-Puig, A., Solanes, G., Grujic, D., Flier, J.S., and Lowell, B.B. (1997). UCP3: An Uncoupling Protein Homologue Expressed Preferentially and Abundantly in Skeletal Muscle and Brown Adipose Tissue. Biochem. Biophys. Res. Commun. *235*, 79–82.

Weber, M., Davies, J.J., Wittig, D., Oakeley, E.J., Haase, M., Lam, W.L., and Schübeler, D. (2005). Chromosome-wide and promoter-specific analyses identify sites of differential DNA methylation in normal and transformed human cells. Nat. Genet. *37*, 853–862.

Weinhold, B. (2006). Epigenetics: The Science of Change. Environ. Health Perspect. *114*, A160–A167.

Wolfe, R.R., and Jahoor, F. (1990). Recovery of labeled CO2 during the infusion of C-1- vs C-2-labeled acetate: implications for tracer studies of substrate oxidation. Am. J. Clin. Nutr. *51*, 248–252.

Wu, Z., Zhang, J., and Zhao, B. (2009). Superoxide Anion Regulates the Mitochondrial Free Ca2+ Through Uncoupling Proteins. Antioxid. Redox Signal. *11*, 1805–1818.

Xiao, M., Yang, H., Xu, W., Ma, S., Lin, H., Zhu, H., Liu, L., Liu, Y., Yang, C., Xu, Y., et al. (2012). Inhibition of α-KG-dependent histone and DNA demethylases by fumarate and succinate that are accumulated in mutations of FH and SDH tumor suppressors. Genes Dev. *26*, 1326–1338.

Xie, C., Naito, A., Mizumachi, T., Evans, T.T., Douglas, M.G., Cooney, C.A., Fan, C.-Y., and Higuchi, M. (2007). Mitochondrial regulation of Cancer Associated Nuclear DNA Methylation. Biochem. Biophys. Res. Commun. *364*, 656–661.

Xu, W., Yang, H., Liu, Y., Yang, Y., Wang, P., Kim, S.-H., Ito, S., Yang, C., Wang, P., Xiao, M.-T., et al. (2011). Oncometabolite 2-Hydroxyglutarate Is a Competitive Inhibitor of α-Ketoglutarate-Dependent Dioxygenases. Cancer Cell *19*, 17–30.

Yasuno, K., Ando, S., Misumi, S., Makino, S., Kulski, J.K., Muratake, T., Kaneko, N., Amagane, H., Someya, T., Inoko, H., et al. (2007). Synergistic association of mitochondrial uncoupling protein (UCP) genes with schizophrenia. Am. J. Med. Genet. B Neuropsychiatr. Genet. *144B*, 250–253.

Yu, X.X., Mao, W., Zhong, A., Schow, P., Brush, J., Sherwood, S.W., Adams, S.H., and Pan, G. (2000). Characterization of novel UCP5/BMCP1 isoforms and differential regulation of UCP4 and UCP5 expression through dietary or temperature manipulation. FASEB J. *14*, 1611–1618.

Žáčková, M., Škobisová, E., Urbánková, E., and Ježek, P. (2003). Activating ω-6 Polyunsaturated Fatty Acids and Inhibitory Purine Nucleotides Are High Affinity Ligands for Novel Mitochondrial Uncoupling Proteins UCP2 and UCP3. J. Biol. Chem. *278*, 20761–20769.

Zaretskaia, M.V., Zaretsky, D.V., Shekhar, A., and DiMicco, J.A. (2002). Chemical stimulation of the dorsomedial hypothalamus evokes non-shivering thermogenesis in anesthetized rats. Brain Res. *928*, 113–125.

Zhang, C.-Y., Baffy, G., Perret, P., Krauss, S., Peroni, O., Grujic, D., Hagen, T., Vidal-Puig, A.J., Boss, O., Kim, Y.-B., et al. (2001). Uncoupling Protein-2 Negatively Regulates Insulin Secretion and Is a Major Link between Obesity, β Cell Dysfunction, and Type 2 Diabetes. Cell *105*, 745–755.